6-2011

Comparative Study of Aerosols Using Particle Induced X-Ray Emission

Colin L. Gleason
Union College - Schenectady, NY

Comparative Study of Aerosols Using Particle Induced X-Ray Emission

Colin Gleason

March 17, 2011

* * * * * * * * *

Submitted in partial fulfillment

of the requirements for

Honors in the Department of Physics and Astronomy

UNION COLLEGE

June, 2011

Abstract

A comparative study of atmospheric aerosols was performed on samples collected in Schenectady, NY using Particle Induced X-ray Emission (PIXE) spectroscopy. PIXE is an elemental analysis technique used to measure the elemental concentration of a sample. This is part of a systematic study to identify the sources and understand the transport, transformation, and effects of airborne pollutants and the connection between aerosols, the deposition of pollution, and the uptake of pollutants by wildlife and vegetation. The atmospheric aerosols were collected with a nine-stage cascade impactor that allows for the analysis of the particulate matter as a function of particle size. The samples were bombarded with 2-MeV proton beams from the Union College Pelletron Accelerator and the energy spectra of the X-rays were measured with a silicon drift detector. The X-ray spectra were analyzed using GUPIX software to extract the elemental concentrations of the particulate matter. The sample collection and analysis are described, and results are presented.

Contents

1 Introduction **1**

2 PIXE Technique **3**

3 Experimental Procedure **5**

3.1 Sample Collection 5

3.2 Union College Ion-Beam Analysis Laboratory 9

4 Analysis **10**

5 Results **16**

6 Summary **51**

1 Introduction

Particle induced X-ray Emission (PIXE) spectroscopy is an ion-beam analysis (IBA) technique used to determine the elemental composition of a sample. PIXE is used for elemental analysis because it can detect a broad range of elements from sodium to uranium with high sensitivity and low detection limits, it is non destructive, requires little to no sample preparation, and has short analysis times. PIXE can be simultaneously used with other ion-beam analysis techniques such as proton elastic scattering analysis (PESA), Rutherford back scattering (RBS) analysis, and proton induced gamma ray emission (PIGE) spectroscopy to provide a quantitative analysis of nearly all elements on the periodic table.

In this thesis, I used PIXE to perform a comparative study of aerosols. Samples taken at the Vale Cemetery crematorium are compared to samples collected at the Union College Boathouse in Schenectady, NY. Specifically, I compared samples taken at Vale Cemetery in the summer of 2010 to the samples collected in the winter of 2010 and to the samples collected at the Boathouse during the summer of 2009. The goal of this work is to identify any similarities and differences between the samples, identify possible sources of pollution, and look for any heavy metals that may be toxic. The samples were collected using a nine stage cascade impactor and were analyzed using proton beams with energies around 2 MeV generated by the Union College Pelletron Accelerator.

Atmospheric aerosols, also known as particulate matter, are small particles suspended in the air. Aerosols are produced by both natural and man made sources, such as soil, sea spray, forest fires, coal combustion, and the burning of motor vehicle fuel. While these are just a few sources of aerosol production, aerosols as a whole have a major environmental impact on our world today. They affect our climate by contributing to the development of acid rain, the haze surrounding industrial cities, and global warming. Aerosols directly influence the climate by both reflecting and

absorbing radiation from the sun [1]. They can also modify the structure of clouds by changing their reflectivity. A study led by NASA in 2009 concluded that aerosols may account for at least 45 percent of the global warming experienced by the arctic [1]. The main aerosols that contribute to this are sulfates and black carbon which are both products of human activities. Sulfates are produced by the burning of coal and oil, while black carbon is produced through various industrial processes and the burning of diesel and bio-fuels. It is important to study aerosols and their sources in order to have a better understanding of the transportation, transformation, and effects of pollution throughout the environment.

In addition to having a major environmental impact, certain aerosols are commonly known to have adverse effects on human health and well being. One example of this is exposure to lead, which was a component of automobile gasoline, before its eventual removal in the 1970's. Early exposure to lead in life, even in the very modest of amounts, can cause a decrease in learning ability, IQ, and memory in children [2]. In adults it can create kidney, cardiovascular, and blood pressure problems. In 2008, the EPA lowered the limit for the concentration of lead allowed in the air to 0.15 $\mu g/m^3$. This has been the first change to the standard since 1978 and is ten times lower than the previous limit.

Another element known to be toxic to human health is mercury. One concern is that mercury may be emitted during the cremation process from mercury amalgam fillings [3]. Cremations have risen in America from 5% in 1972 to 35% in 2005, and are expected to continue to rise. Each cremation is believed to release between two and four grams of mercury and the highest observed emission was 8.6 grams in Switzerland [3]. Most of the mercury emitted gets released into the air while a small percentage of it gets deposited in the soil and along the walls of the oven and chimney of the crematorium. One goal of this study is to determine if lead and mercury can be identified in the aerosol samples and, if they are present, then to determine their

elemental concentrations.

2 PIXE Technique

PIXE is an analysis technique used to measure the elemental concentration of a sample [4]. Shown in Figure 1 is a typical experimental setup used for PIXE. Proton beams generated by an ion accelerator bombard a thin sample and produce X-rays that can be detected. The protons that do not interact with the sample pass through it and are collected in the Faraday cup. Figures 2 and 3 illustrate how the X-rays are produced. An incident proton will occasionally knock an inner shell electron out of the atom, creating a vacancy. An outer shell electron will fill the void, emitting an X-ray that can be detected. Each element has a characteristic X-ray spectrum which allows for the identification of nearly all elements present in the sample. The concentration of an element is determined from the intensities of the detected X-rays.

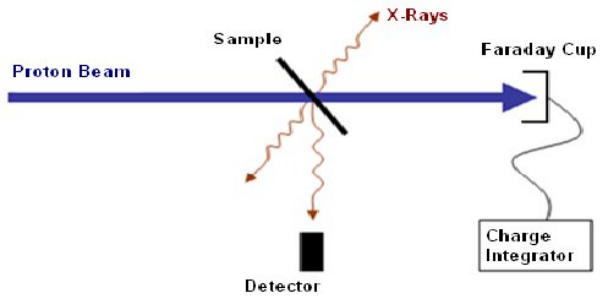

Figure 1: A schematic for a basic PIXE experimental setup for thin targets.

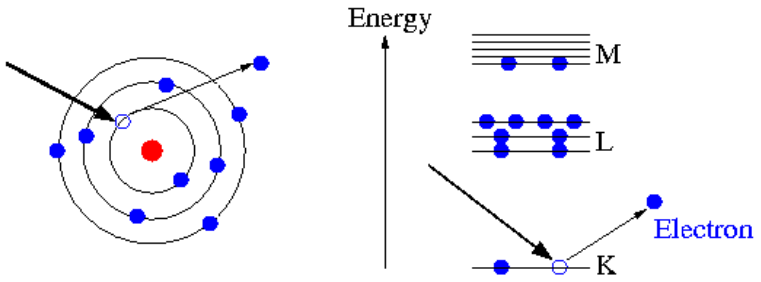

Figure 2: An incident proton knocks an inner shell electron out of the atom.

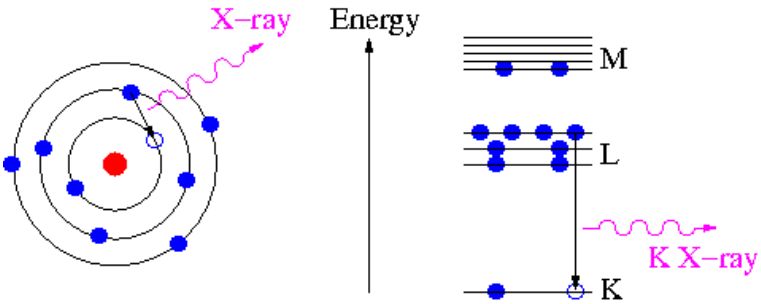

Figure 3: An outer shell electron fills the hole that was created when an inner shell electron is ejected. This results in the production of an X-ray.

The concentration C_Z of an element Z present in the sample is given by

$$C_z = \frac{Y_z}{Y_t \cdot H \cdot Q \cdot \epsilon \cdot T} \tag{1}$$

where Y_z is the intensity of the principle X-ray line for element Z, Y_t is the theoretical intensity per micro-Coulomb of charge, H is an experimental constant determined by taking data on a set of standards, Q is the measured beam charge incident on the sample, ϵ is the intrinsic efficiency of the detector, and T is the coefficient for transmission through any filters or absorbers between the target and the detector. These parameters are either known or determined during the PIXE analysis.

3 Experimental Procedure

3.1 Sample Collection

A nine-stage cascade impactor was used to collect the aerosols and separate them based on their particle size [5]. Shown in Figure 4 is a schematic and photograph of the impactor. Aerosols drawn through the impactor become impacted on thin kapton foils in nine different stages. When air is drawn through the impactor at a rate of 1 L/min, each stage collects aerosols of different diameter ranges: >16μm , 16-8 μm, 8-4 μm, 4-2 μm, 2-1 μm, 1.0-0.5 μm, 0.5-0.25 μm, 0.25-0.12 μm, and 0.12-0.06 μm. A tenth stage, known as the after filter, collects aerosols < 0.06 μm. Photographs of a kapton foil and microscopic images of aerosol deposits are shown in Figure 5 . The microscopic photographs are for aerosols of 0.5-0.25 μm, 0.5-0.25 μm, 4-2 μm, and 8-4 μm for the top row and 0.5-0.25 μm, 1.0-0.5 μm, and 4-2 μm in diameter for the bottom row, respectively. The kapton foils are then used as targets in the PIXE experiments with the accelerator.

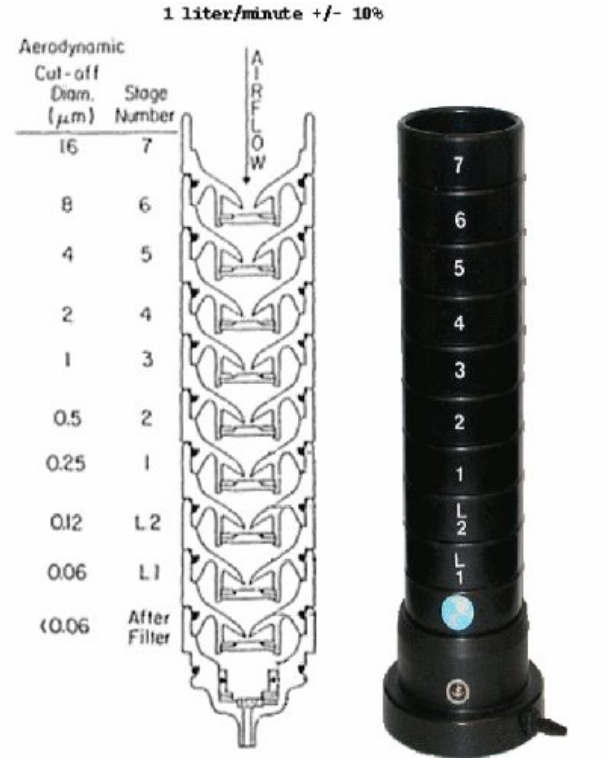

Figure 4: A cross section and photograph of the nine-stage cascade impactor that was used to collect the aerosol samples.

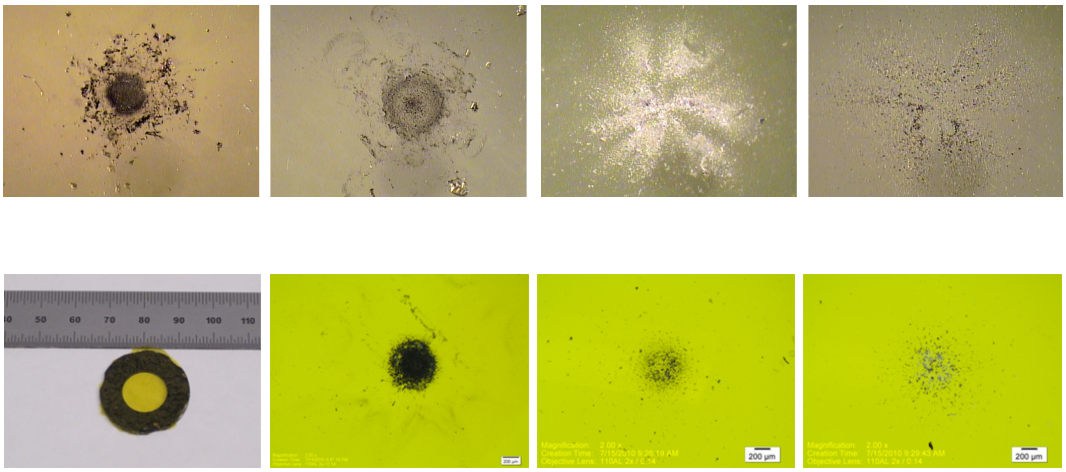

Figure 5: A photograph of a kapton impaction foil and several microscopic images of various aerosol deposits. The microscopic photographs are for aerosols of 0.5- 0.25 µm, 0.5-0.25 µm, 4-2 µm, and 8-4 µm for the top row and 0.5-0.25 µm, 1.0-0.5 µm, and 4-2 µm in diameter for the bottom row, respectively.

The samples were collected at the Vale Cemetery crematorium and at the Union College Boathouse along the Mohawk River in Schenectady, New York. The samples collected at Vale Cemetery were taken during the winter of 2010 as well as during the summer of 2010 while the samples collected at the Union College Boathouse were collected during the summer of 2009. Shown in Figure 6 is a photograph of the nine stage cascade impactor on the roof of the Vale Cemetery crematorium when samples were being collected. Figure 7 is a photograph of the impactor with all the necessary pieces of equipment needed to collect samples labeled. The pump, which is connected to a power source, draws air through the impactor. The flow rate is controlled by the valve and is monitored using the flow meter. The flow rate was regularly monitored in order to ensure that the flow rate of 1 L/min was maintained. The samples were collected for periods of approximately 48 hours which corresponds to a total of 2.7 m^3 of air that flows through the impactor.

Figure 6: A photograph of the impactor collecting samples on the roof of the Vale Cemetery crematorium.

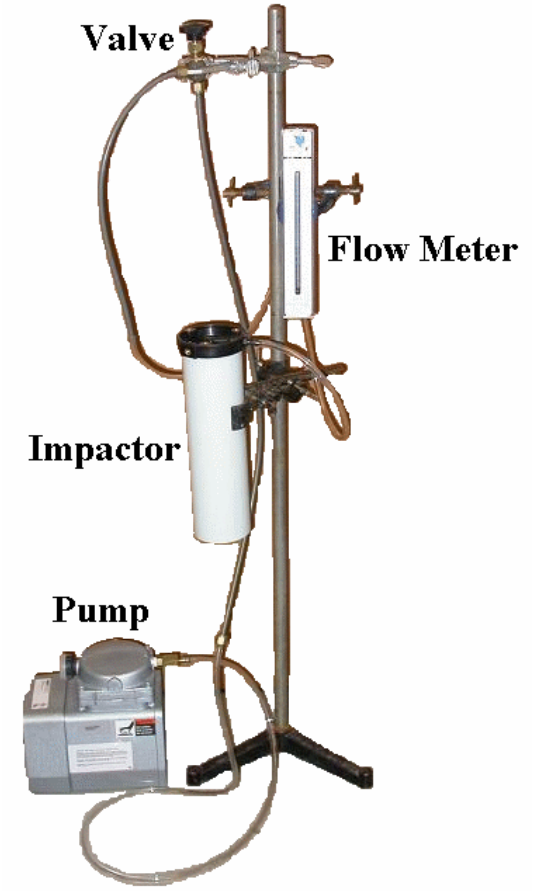

Figure 7: An image of the nine stage cascade impactor and all the components necessary for aerosol sampling.

3.2 Union College Ion-Beam Analysis Laboratory

The PIXE experiments were conducted in the Union College Ion-Beam Analysis Laboratory (UCIBAL). The main instrument in the UCIBAL is the 1.1-MV Pelletron Accelerator shown in Figure 8. Protons were generated at the source and accelerated to energies up the 2.2 MeV in the accelerator tank. The beam then traveled through the quadrupole and switcher magnets which focused and steered the beam of protons towards the scattering chamber.

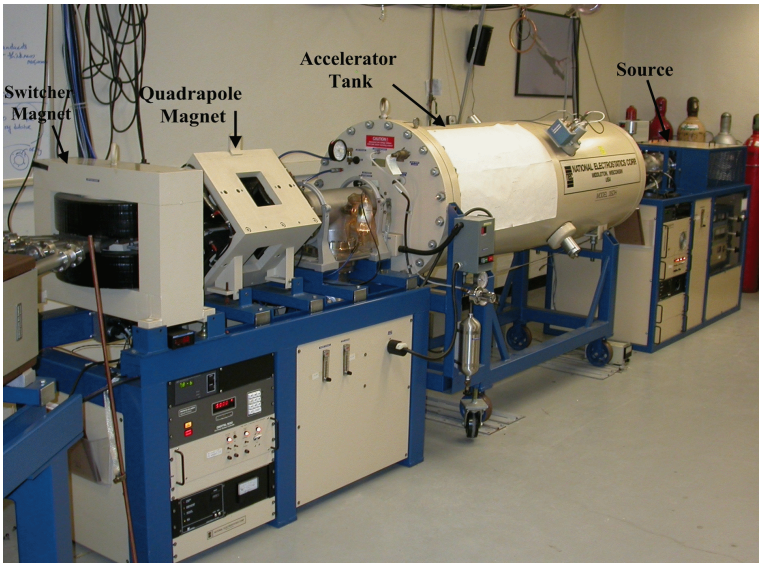

Figure 8: A photograph of the Union College Pelletron Accelerator.

Located at the end of the accelerator was the scattering chamber, shown in Figure 9. Proton beams of 2 mm in diameter were incident upon samples which were at an angle of 45° relative the the beam. Emitted X-rays were collected by the Silicon Drift Detector (SDD) [6] which was at an angle of 90 degrees relative to the proton beam. An ^{241}Am source was used to calibrate the SDD detector. The majority of the protons did not interact with atoms in the sample. These protons simply passed through the samples and were collected by the Faraday cup, which was connected to a charge integrator. The charge integrator measured the amount of charge incident on the target. Beam currents of 5 to 10 nA were used in the experiments. The signals

from the SDD were processed with the Amptek PX4 Digital Pulse Processor and the energy spectra were acquired with Amptek Analog and Digital acquisition software [6]. Energy spectra were taken on aerosols collected at the Union College Boathouse in the summer of 2009 and at Vale Cemetery in the summer and winter of 2010. Spectra were also taken on a set of standards to determine the experimental H-value in Eq. (1) [7]. These spectra show the intensity of the measured X-rays versus the X-ray energy.

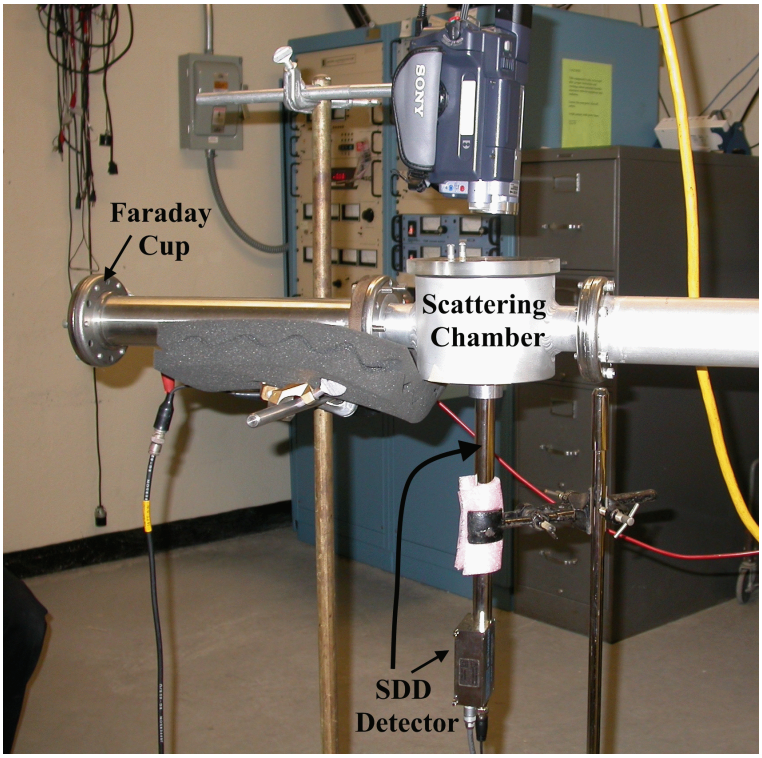

Figure 9: A photograph of the scattering chamber, SDD detector, and Faraday cup.

4 Analysis

The X-ray spectra collected by the SDD were analyzed using GUPIX , a software package specifically designed for fitting PIXE spectra [8]. GUPIX works by extracting the X-ray peak intensities from the background spectra and then converts those intensities to elemental concentrations in mass per unit area (ng/cm^2). A spectrum

and various experimental parameters such as the H-value, the proton beam energy, the total charge measured in the Faraday cup, and energy calibration parameters were loaded into GUPIX to perform an accurate fit. Initially, GUPIX is able to recognize elemental peaks in the spectra, as shown in Figure 10. To perform a fit to the data, which determines the elemental concentrations, a list of elements was placed into another set of parameters.

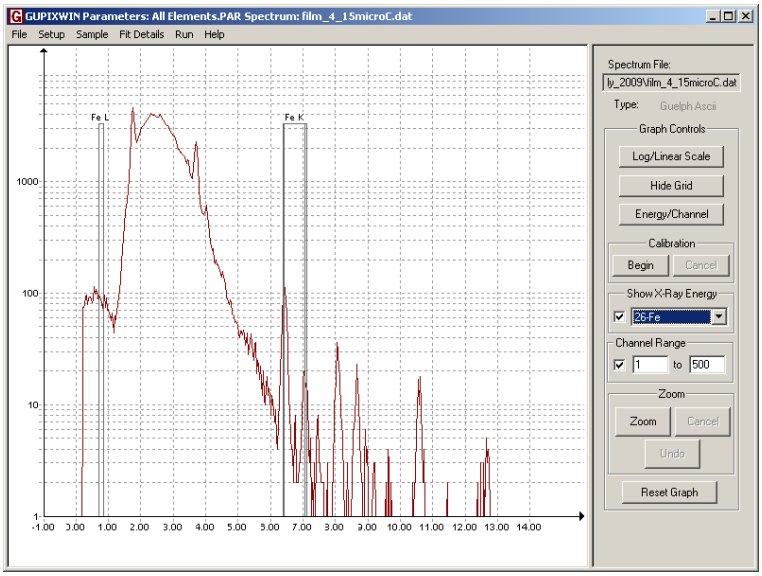

Figure 10: An X-ray spectrum for particulate matter between 2-4 μm loaded in GUPIX, a software program used to fit the peaks and determine the elemental concentrations.

After all the parameters and elements were inputted, GUPIX was able to perform a fit to the data, as shown in Figure 11. This is a fitted PIXE spectrum for aerosols between 0.25-0.5 μm in diameter collected at the Union College Boathouse. The plot displays the number of X-ray counts for each X-ray energy. The blue dots are the individual data points of the measured X-rays and the red line is the GUPIX fit to the data. Table 1 shows the elemental concentrations that GUPIX generated for this sample. Also presented in Table 1 are the statistical and fit errors. These errors are part of the error analysis for the final concentrations.

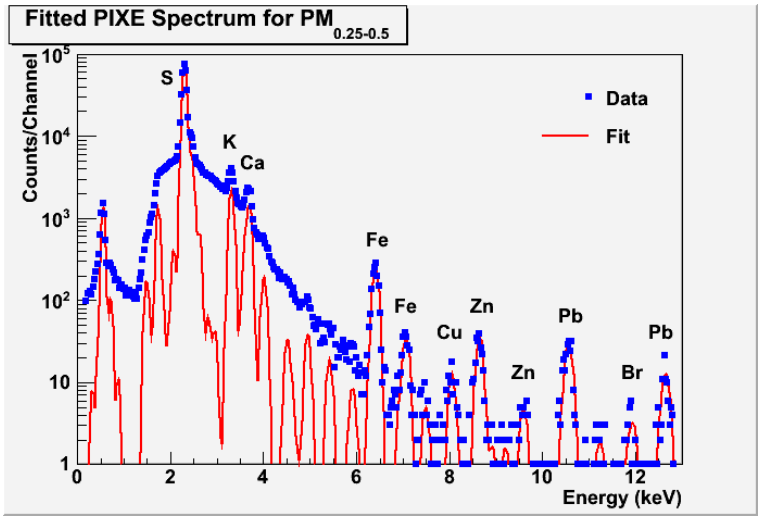

Figure 11: A GUPIX fit to a PIXE spectrum for aerosols between 0.25-0.5 μm collected at the Union College Boathouse.

Table 1: Concentrations in ng/cm^2 for all elements in the GUPIX analysis of Figure 11.

Z	Element	Conc. (ng/cm^2)	% Stat Error	% Fit Error
13	Al	188	17	27
14	Si	319	4	9
16	S	4430	0.2	3
17	Cl	39	12	16
19	K	154	2	3
20	Ca	99	3	4
22	Ti	3	45	38
23	V	5	29	24
24	Cr	3	40	34
25	Mn	5	22	20
26	Fe	92	3	4
27	Co	1	140	98
28	Ni	4	25	25
29	Cu	9	18	16
30	Zn	35	9	9
34	Se	4	81	80
35	Br	4	120	120
38	Sr	5	130	260
82	Pb	185	10	18

In order for the GUPIX concentrations to be accurate, the H-value has to be found. The process of determining the H-value is fairly straightforward and if the charge

integration for our system is perfect, then H should simply be the solid angle of the detector. The H-value should be constant over all elements and not vary by atomic number. The first step in determining H was to take PIXE spectra on 16 MicroMatter single element standards with known elemental concentrations [7]. Shown in Figure 12 is a PIXE spectrum of a 6.3 μm thick Iron MicroMatter standard with a known concentration of 45.1 $\mu g/cm^2 \pm 5\%$. The energy spectra were then individually analyzed in GUPIX with an initial H-value set arbitrarily to one. The result of this was an elemental concentration that was much less than the known concentration. To find the real H-value of the system, a ratio was taken of this concentration to the known concentration. Shown in Figure 13 is a plot of the H-value as a function of atomic number for the single elemental standards. The average H-value was 0.0024 with a maximum of 6% variation.

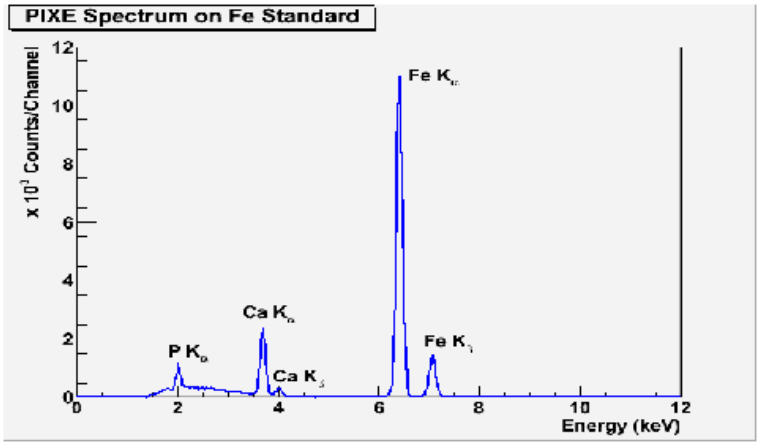

Figure 12: A PIXE spectrum of an Fe MicroMatter standard used for calibration purposes.

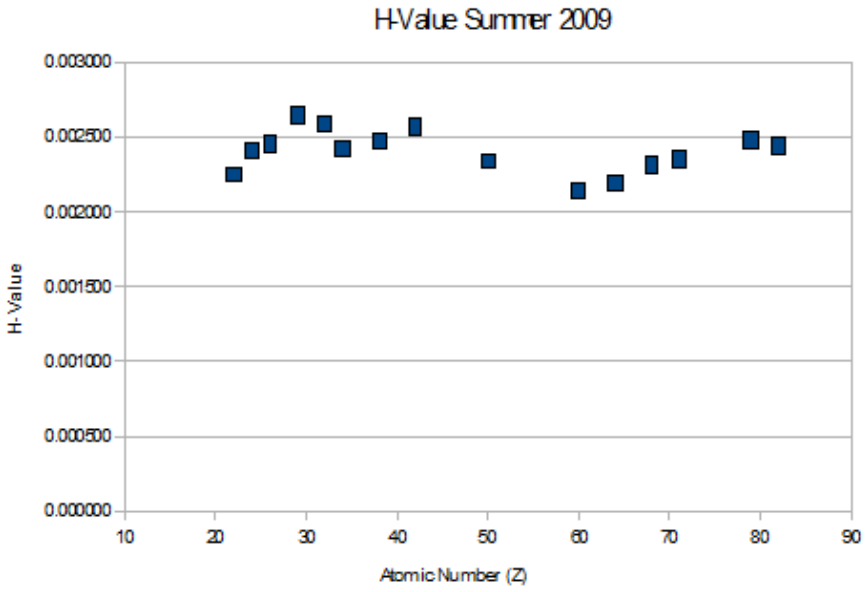

Figure 13: A plot of the H-value as a function of atomic number for single element standards taken during the Summer of 2009.

The elemental concentrations of the aerosols calculated by GUPIX were then converted from mass per unit area on the kapton foils to mass per unit volume in air. Since GUPIX measures the concentration that is deposited on the kapton foil, the conversion determines elemental concentration in the air that was sampled. The concentration of an element Z in ng/m^3 is given by

$$Conc.\left(ng/m^3\right) = \frac{P_{std}}{T_{std} \cdot \Delta t} \cdot \frac{Conc.(ng/cm^2) \cdot A \cdot T}{P \cdot f} \tag{2}$$

where P_{std} is the standard pressure given at 760 mm Hg, T_{std} is the standard temperature given at 25°C, Δt is the amount of time it took to collect the samples, $Conc.\ (ng/cm^2)$ is the concentration determined by GUPIX, A is the area of the deposit on the kapton foil, T is the average temperature during sampling, P is the average pressure during sampling, and f is the average flow rate of air that is being pulled through the impactor.

The average pressure and temperature of the local weather were recorded during

the sampling period. This meant that the only two parameters in Eq. (2) that needed to be determined were the concentration in ng/cm^2 (as described above) and the area of the aerosol deposit. The areas of the deposits were found by taking microscopic images of the deposits then using multiple estimates of the area to find an average value. Figure 14 is a photograph showing how these measurements were taken for stage 4 (aerosols between 2-4 μm) of the Union College Boathouse samples. First, an initial estimate of the aerosol deposit was made that encompasses nearly all visible components of the deposit (red circle #1). A second measurement was then made that encompassed an area slightly smaller than the full aerosol deposit (red circle #2). Finally, a third measurement was made that was smaller than the second measurement that encompassed the areas that have highest aerosol deposit concentration (red circle #3). Once this was completed, the mean area was used in Eq. (2) to calculate the elemental concentration in mass per unit volume of air sampled.

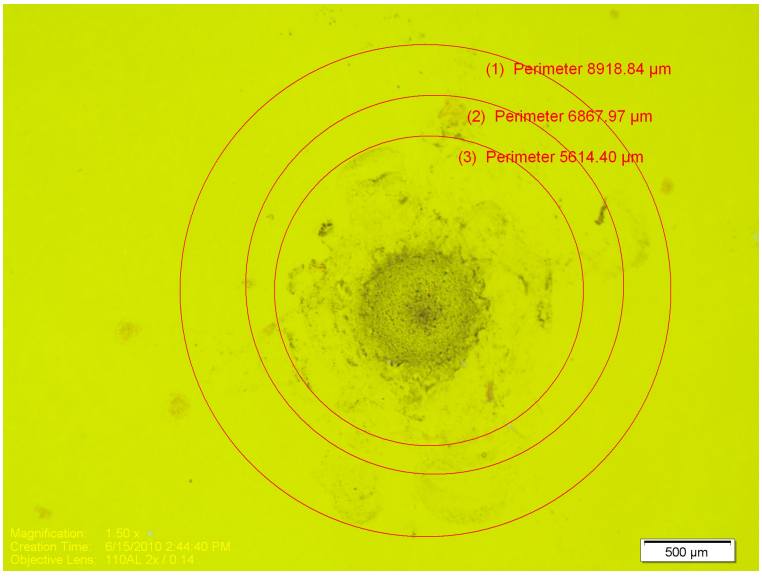

Figure 14: A photograph of the three measurements used to determine the area of the aerosol deposit on Stage 1 of the Union College Boathouse samples.

5 Results

PIXE spectra were taken for all stages of both Vale Cemetery samples and for Stages 1, 2, 4-7 for the Union College Boathouse sample. Stage 3 of the Boathouse sample was not analyzed because a mosquito was impacted on the kapton foil which prevented the analysis of the sample. Concentrations for Stages L1 and L2 for the Boathouse sample are also not shown because the X-ray spectra do not differ from the blank kapton foils. This means that there were no aerosols impacted on the kapton foils or that the proton beam did not hit the aerosol deposits. Shown in Figure 15 are PIXE spectra comparing an impacted kapton foil for particles between 2-4μm collected at the Union College Boathouse to a blank kapton foil. The graph displays the number of counts for each energy of X-ray measured. The purpose of this graph is to show that the aerosols on the kapton foil were hit by the proton beam and that the elements measured were distinguishable from both the background and other elements.

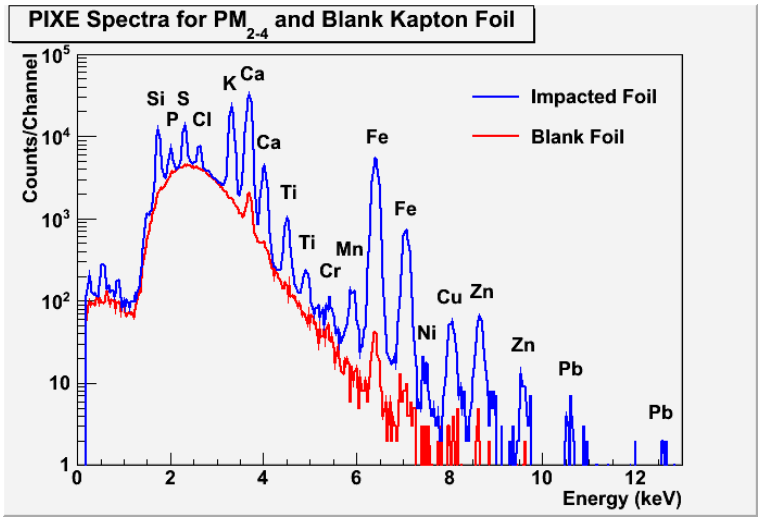

Figure 15: PIXE spectra comparing an impacted kapton foil for particles between 2-4μm (blue) collected at the Union College Boathouse and a blank kapton foil (red).

Shown in Tables 2, 3, and 4 are the elemental concentrations in ng/cm^2 for all samples as determined by GUPIX. Bar graphs comparing the concentrations in ng/cm^2 of samples collected at Union College Boathouse and the summer Vale Cemetery

samples are shown in Figures 16-21. Figures 22-30 show bar graphs comparing the elemental concentrations of the samples collected at Vale Cemetery in the summer to Vale Cemetery in the winter. Figures 16-30 highlight the elemental differences before Eq. (2) was applied to get the concentrations in ng/m^3. The error bars in these graphs were determined by adding the fit error and statistical error determined by GUPIX in quadrature.

Table 2: Elemental concentrations in ng/cm^2 for the Union College Boathouse samples.

Elemental Concentrations (ng/cm^2)						
	Stage 1	2	4	5	6	7
Element	0.25-0.5 μm	0.5-1	2-4	4-8	8-16	>16
Al	157 ±45	229 ±47	640 ±64	718 ±68	321 ±48	128 ±44
Si	232 ±24	476 ±28	2075 ±57	2564 ±66	1133 ±42	328 ±22
S	3700 ±120	1120 ±34	504 ±12	431 ±11	114.3 ±7.4	28.7 ±6.3
Cl	28.7 ±6.1	40.6 ±5.7	190 ±7	163 ±6	41.4 ±5.1	11.1 ±4.8
K	111 ±5	88.1 ±4.2	1075 ±14	1050 ±14	284.4 ±7.7	89.7 ±4.1
Ca	84.6 ±4.0	167.4 ±5.4	1863 ±23	2685 ±32	1305 ±29	431 ±11
Ti	3.2 ±1.5	13.5 ±1.7	82.7 ±2.8	93.4 ±3.0	33.9 ±2.1	6.1 ±1.6
Cr	2.8 ±1.2	4.2 ±1.2	6.9 ±1.6	9.3 ±1.7	4.1 ±1.3	1.1 ±1.1
Fe	73.8 ±3.9	254 ±8	1525 ±21	1472 ±20	446 ±12	67.5 ±3.4
Ni	2.3 ±1.1	0.1 ±0.9	6.9 ±1.6	1.6 ±1.4	1.1 ±0.9	1 ±0.9
Cu	8.3 ±1.9	8.6 ±1.9	34.9 ±3.6	18.8 ±2.7	3.6 ±1.4	0.1 ±0.9
Zn	32.1 ±3.8	6.1 ±2.0	55.9 ±4.8	40.5 ±4.2	16.5 ±2.8	9.5 ±2.2
Se	6.8 ±4.3	5.3 ±3.8	0 -	0 -	0 -	0 -
Br	15.2 ±7.2	6.7 ±5.4	4.5 ±4.6	0 -	0 -	0 -
Pb	210 ±60	17 ±27	30 ±34	0 -	0 -	0 -

Table 3: Elemental concentrations in ng/cm^2 for aerosols collected at Vale Cemetery during the summer of 2010.

Elemental Concentration (ng/cm^2)									
Element	Stage L1	L2	1	2	3	4	5	6	7
Al	169 ±54	195 ±56	164 ±64	286 ±56	320 ±62	322 ±66	387 ±68	287 ±59	68 ±55
Si	129 ±25	144 ±25	284 ±29	336 ±28	607 ±36	815 ±43	928 ±48	640 ±42	115 ±30
S	157 ±16	195 ±19	3132 ±73	767 ±30	347 ±15	231 ±12	164 ±10	97.8 ±9.4	18.9 ±8.1
Cl	81 ±9	114 ±11	451 ±13	23.1 ±5.9	106 ±7	165 ±8	196 ±9	176 ±10	7 ±5
K	186 ±16	232 ±20	1588 ±33	81.5 ±4.6	252.8 ±8.9	461 ±14	339 ±11	207.9 ±9.4	21.7 ±4.7
Ca	110 ±10	161 ±14	209.9 ±7.2	217 ±8	862 ±25	1687 ±45	1875 ±54	1250 ±48	79 ±12
Ti	4.8 ±1.8	2.1 ±1.6	12.6 ±1.9	21.3 ±2.2	48.6 ±2.8	75.9 ±3.4	79.5 ±3.6	47.7 ±3.1	0 -
V	0 -	0 -	2.2 ±1.7	0 -	0 -	0 -	0 -	2.2 ±1.8	1.5 ±1.5
Cr	1.5 ±1.3	3.2 ±1.2	3.1 ±1.4	2.9 ±1.3	6.3 ±1.4	6.6 ±1.5	6.9 ±1.5	3.7 ±1.4	2.2 ±1.3
Fe	23.2 ±3.2	32.4 ±4.0	87.6 ±4.5	134.1 ±6.6	387 ±13	455 ±14	368 ±12	203.9 ±9.8	18.9 ±3.7
Co	0 -	0 -	1.8 ±2.7	0 -	0 -	0 -	1.6 ±4.1	0 -	1.5 ±1.4
Ni	0 -	1.6 ±1.2	2.5 ±1.6	2.1 ±1.3	0 -	1 ±1.4	1.3 ±1.2	1 ±1	2.3 ±1.2
Cu	5.9 ±2.2	1.2 ±1.4	11.1 ±2.9	3.7 ±1.7	11.7 ±2.9	12.5 ±2.9	5.7 ±2.1	3 ±1	1.5 ±1.4
Zn	7.5 ±3.1	12.6 ±3.6	171 ±11	7.1 ±2.9	16.8 ±3.8	22 ±4	14.9 ±3.8	14.1 ±3.7	3.9 ±2.1
As	0 -	0 -	0 -	0 -	4.6 ±5.4	3.9 ±4.9	0 -	0 -	0 -
Se	0 -	0 -	5.7 ±6.2	0 -	0 -	0 -	0 -	0 -	0 -
Br	0 -	0 -	24 ±11	5.3 ±7.6	0 -	0 -	0 -	0 -	0 -
Sr	0 -	0 -	0 -	0 -	0 -	13 ±23	0 -	0 -	0 -
Hg	0 -	0 -	0 -	0 -	0 -	4 ±10	0 -	0 -	11 ±11
Pb	0 -	0 -	46 ±29	13 ±23	0 -	0 -	10 ±23	0 -	0 -

Table 4: Elemental concentrations in ng/cm^2 for aerosols collected at Vale Cemetery during the winter of 2010.

Elemental Concentration (ng/cm^2)									
Element	Stage L1	L2	1	2	3	4	5	6	7
Al	3015 ±1120	2517 ±980	3684 ±1170	2578 ±1080	3916 ±1100	8956 ±1220	16740 ±1590	6134 ±1070	2673 ±1051
Si	1766 ±470	2296 ±475	4089 ±456	1620 ±465	5671 ±525	16146 ±702	34240 ±1050	10670 ±614	2182 ±452
S	1097 ±182	1582 ±230	10110 ±386	2510 ±361	2561 ±184	2496 ±198	4123 ±254	1316 ±166	1826 ±192
Cl	3627 ±386	5675 ±631	51337 ±1530	2534 ±347	6881 ±301	38760 ±872	91730 ±1480	25950 ±760	2770 ±214
K	2922 ±319	4657 ±531	38350 ±1100	4379 ±565	1703 ±98	3829 ±117	7982 ±160	2785 ±109	607 ±75
Ca	96 ±150	76 ±160	900 ±122	128 ±177	7402 ±349	27030 ±603	65340 ±1000	20300 ±593	709 ±130
Ti	77 ±31	27 ±29	118 ±33	43 ±31	638 ±47	1832 ±65	3948 ±92	1337 ±60	39 ±31
V	24 ±25	8 ±25	2 ±31	0 -	0 -	87 ±39	122 ±55	9 ±36	11 ±26
Cr	59 ±25	50 ±23	115 ±31	59 ±25	61 ±24	136 ±31	128 ±42	113 ±28	71 ±24
Fe	140 ±45	62 ±35	568 ±50	94 ±39	1523 ±96	5364 ±162	9757 ±211	2857 ±118	1862 ±137
Co	14 ±19	10 ±16	0 -	0 -	0 -	6 ±58	11 ±83	11 ±42	35 ±34
Ni	29 ±18	23 ±18	29 ±23	0 -	35 ±20	25 ±24	109 ±40	22 ±19	21 ±18
Cu	21 ±21	7 ±16	133 ±35	0 -	246 ±45	142 ±36	783 ±77	51 ±25	12 ±18
Zn	114 ±41	216 ±55	2341 ±143	202 ±54	382 ±62	357 ±56	1027 ±98	258 ±59	71 ±31
As	0 -	0 -	0 -	0 -	0 -	23 ±52	23 ±59	0 -	0 -
Se	43 ±60	0 -	0 -	0 -	0 -	0 -	21 ±59	0 -	0 -
Br	0 -	0 -	175 ±114	99 ±101	0 -	52 ±82	0 -	0 -	0 -
Hg	0 -	0 -	0 -	0 -	28 ±99	29 ±114	0 -	87 ±123	0 -
Pb	0 -	0 -	395 ±302	0 -	83 ±260	0 -	52 ±270	0 -	0 -

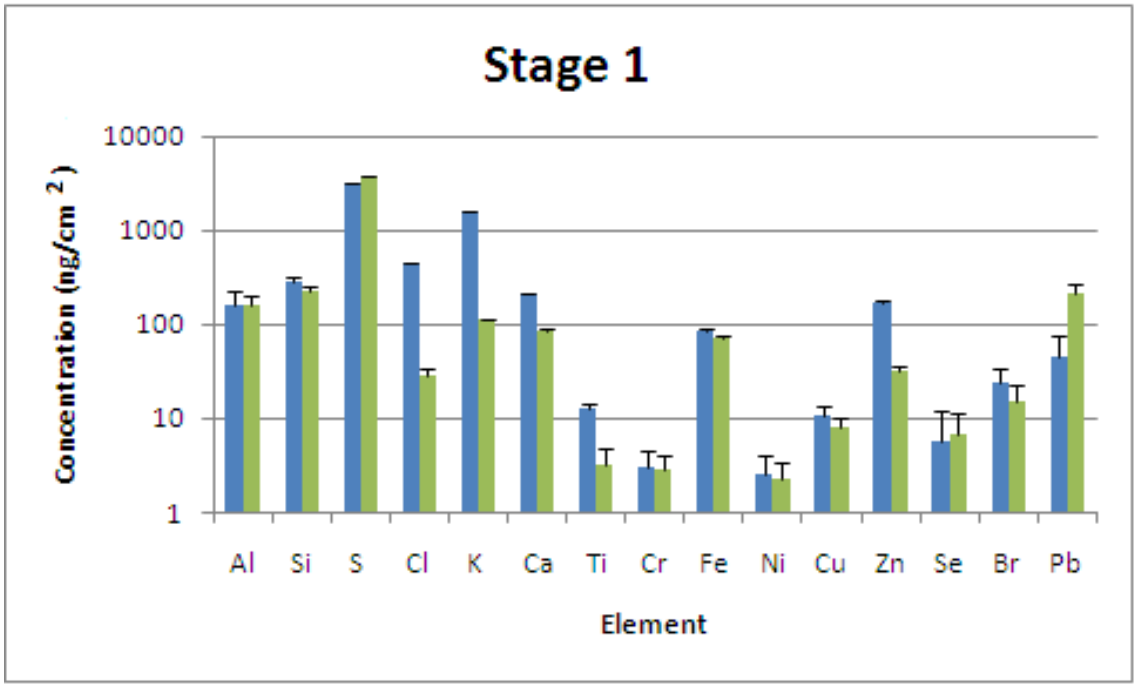

Figure 16: Bar graph comparing the elemental concentrations in ng/cm^{2}of aerosols with a diameter between 0.5-0.25 μm collected at Vale Cemetery in the summer of 2010 (blue) and at the Union College Boathouse (green).

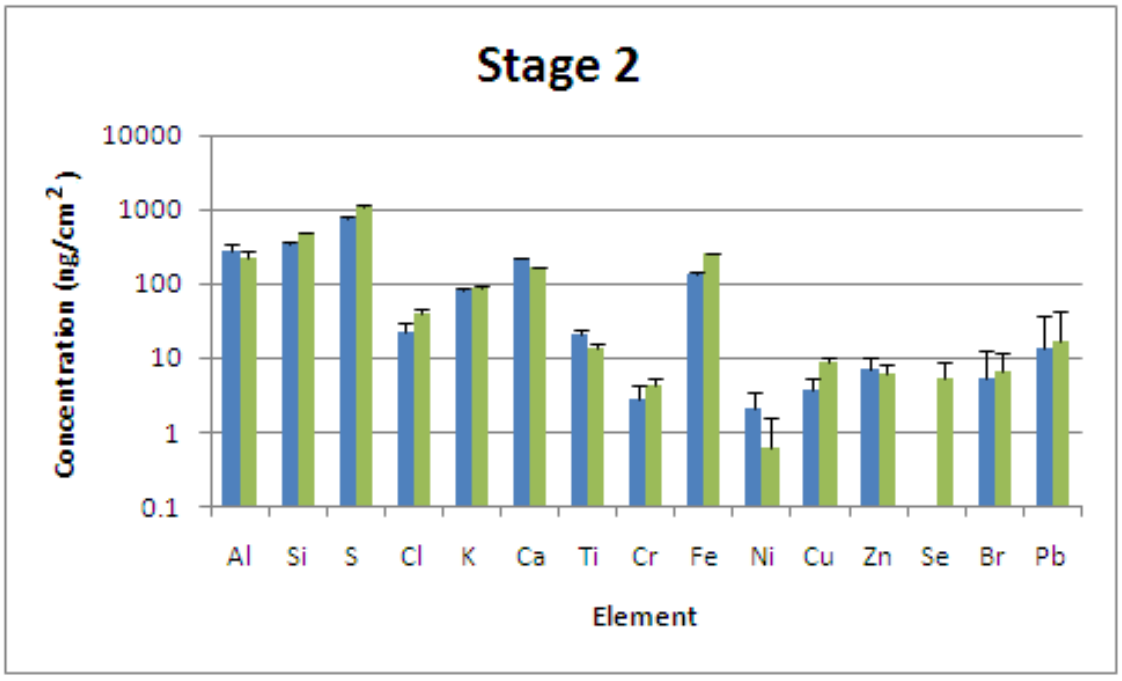

Figure 17: Bar graph comparing the elemental concentrations in ng/cm^{2}of aerosols with a diameter between 1.0-0.5 μm collected at Vale Cemetery in the summer of 2010 (blue) and at the Union College Boathouse (green).

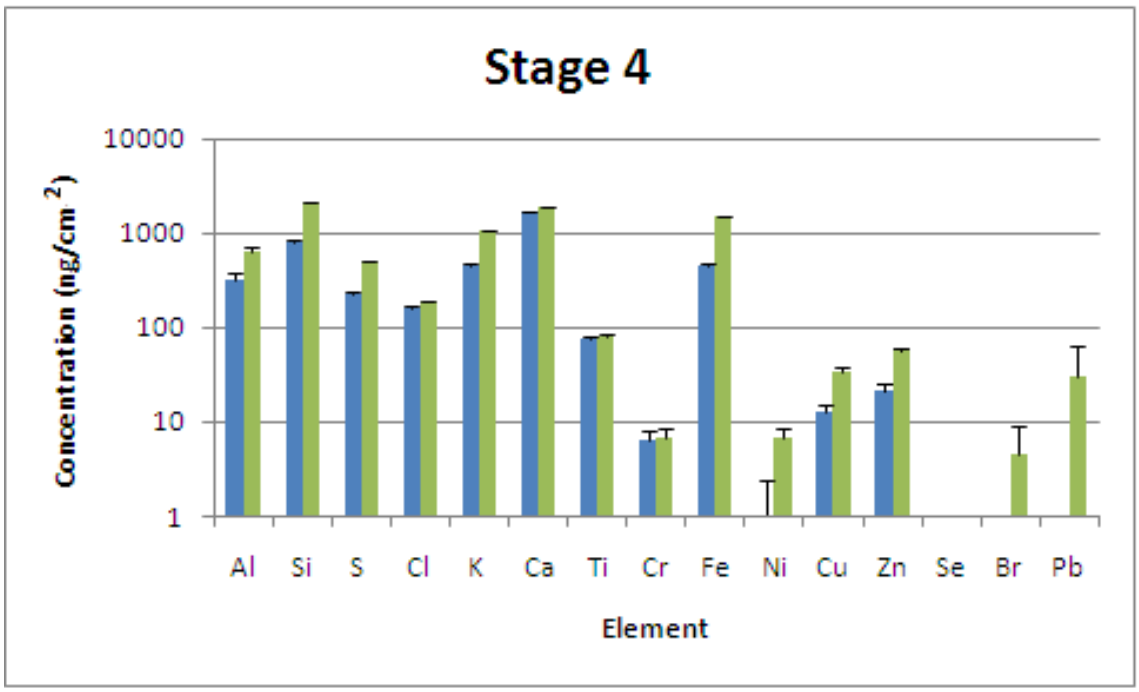

Figure 18: Bar graph comparing the elemental concentrations in ng/cm^{2}of aerosols with a diameter between 4-2 μm collected at Vale Cemetery in the summer of 2010 (blue) and at the Union College Boathouse (green).

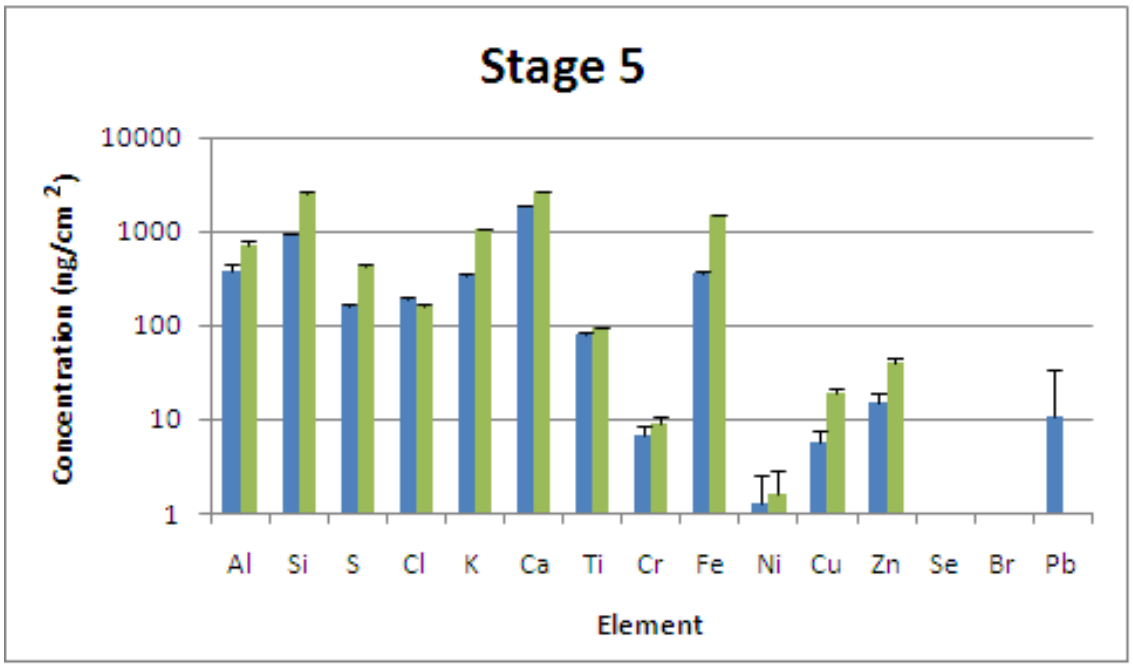

Figure 19: Bar graph comparing the elemental concentrations in ng/cm^{2}of aerosols with a diameter between 8-4 μm collected at Vale Cemetery in the summer of 2010 (blue) and at the Union College Boathouse (green).

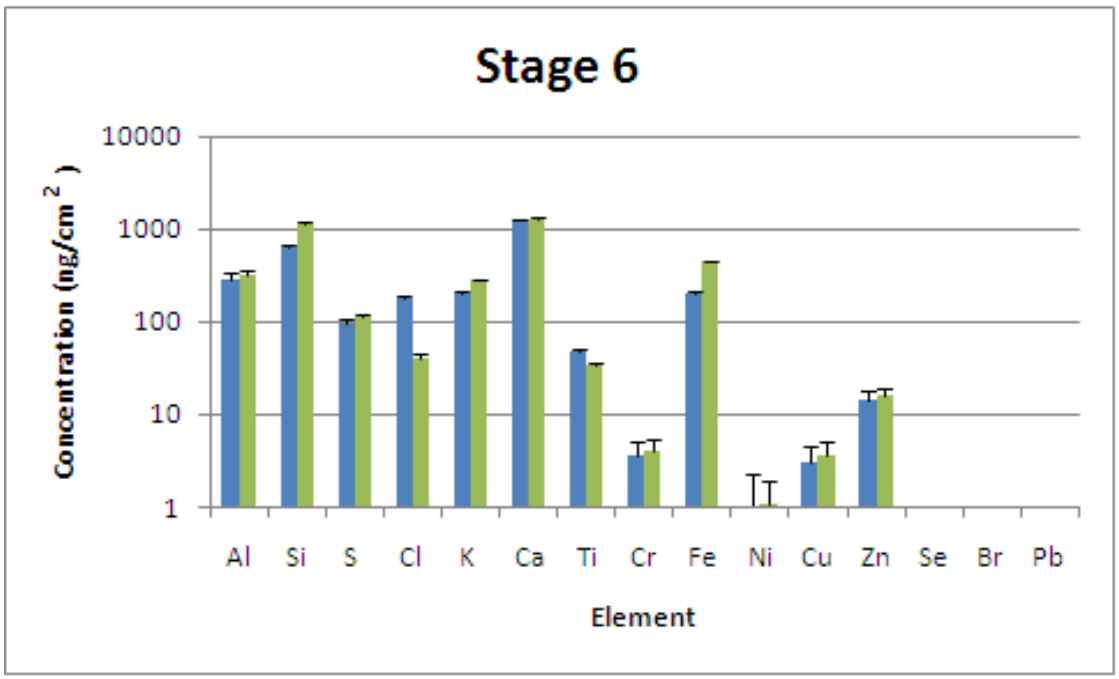

Figure 20: Bar graph comparing the elemental concentrations in ng/cm^{2}of aerosols with a diameter between 16-8 μm collected at Vale Cemetery in the summer of 2010 (blue) and at the Union College Boathouse (green).

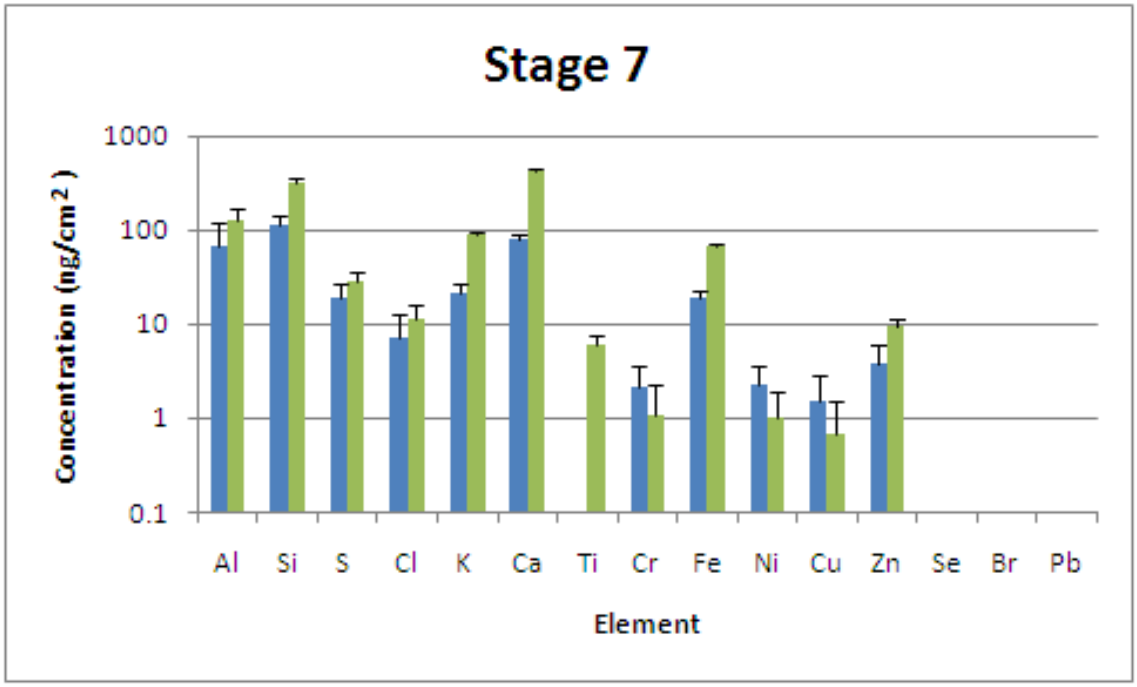

Figure 21: Bar graph comparing the elemental concentrations in ng/cm^{2}of aerosols with a diameter > 16 μm collected at Vale Cemetery in the summer of 2010 (blue) and at the Union College Boathouse (green).

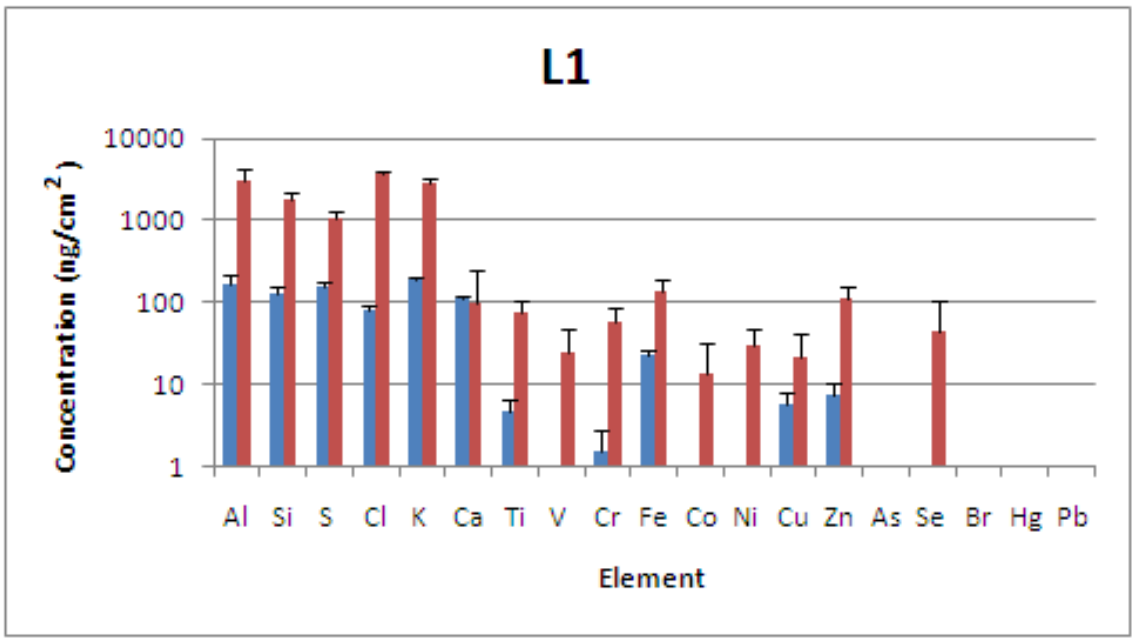

Figure 22: Bar graph comparing the elemental concentrations in ng/cm^{2}of aerosols with a diameter between 0.12-0.06 μm collected at Vale Cemetery in the summer of 2010 (blue) and in the winter of 2010 (red).

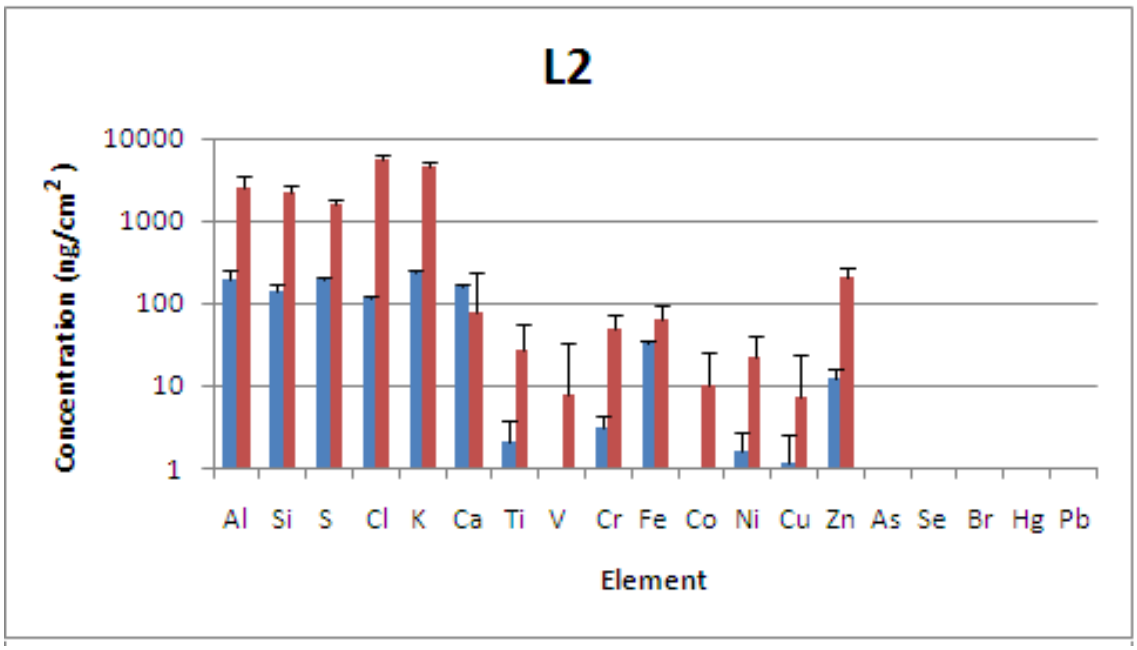

Figure 23: Bar graph comparing the elemental concentrations in ng/cm^{2}of aerosols with a diameter between 0.25-0.12 μm collected at Vale Cemetery in the summer of 2010 (blue) and in the winter of 2010 (red).

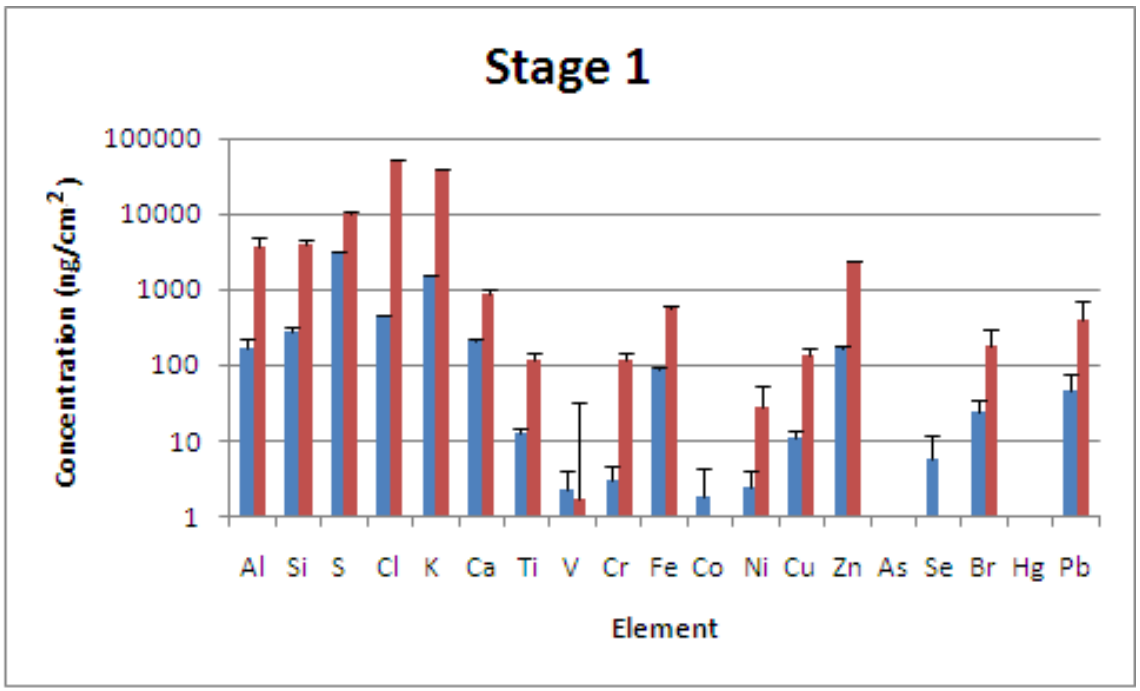

Figure 24: Bar graph comparing the elemental concentrations in ng/cm^{2}of aerosols with a diameter between 0.5-0.25 μm collected at Vale Cemetery in the summer of 2010 (blue) and in the winter of 2010 (red).

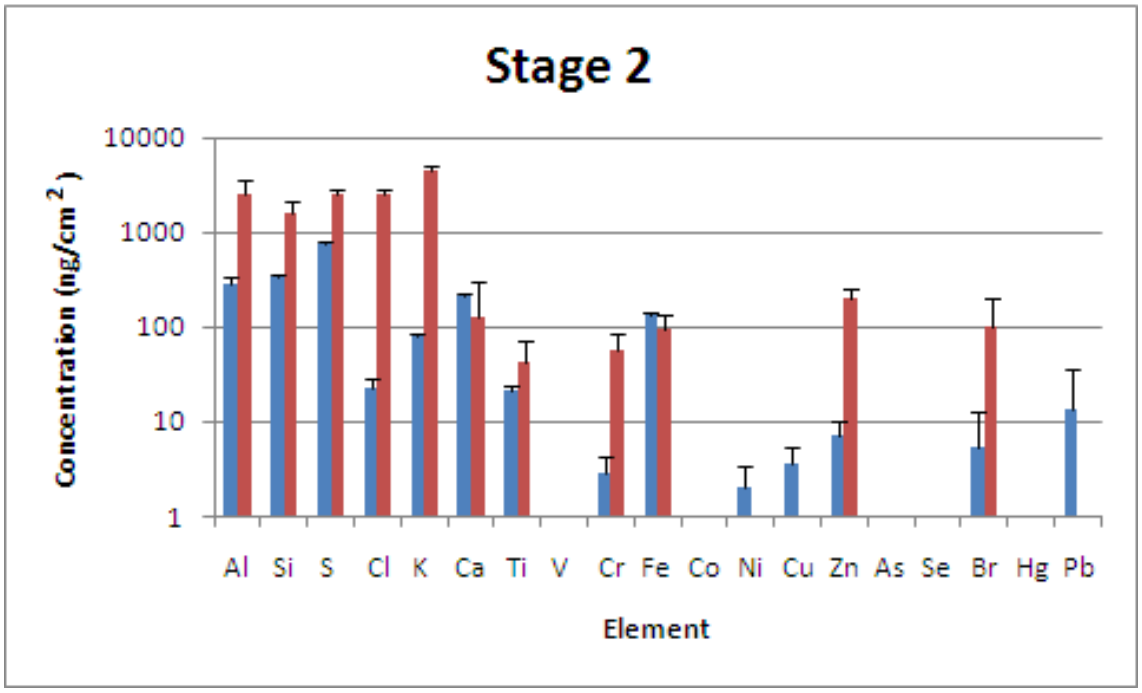

Figure 25: Bar graph comparing the elemental concentrations in ng/cm^{2}of aerosols with a diameter between 1-0.5 μm collected at Vale Cemetery in the summer of 2010 (blue) and in the winter of 2010 (red).

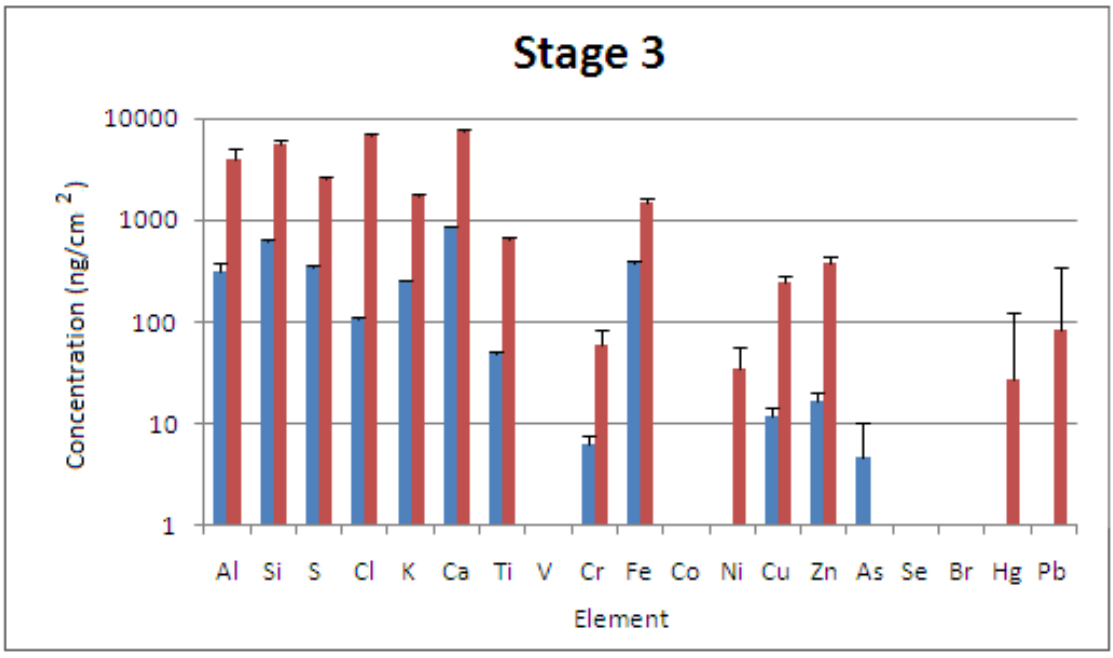

Figure 26: Bar graph comparing the elemental concentrations in ng/cm^{2}of aerosols with a diameter between 2-1 μm collected at Vale Cemetery in the summer of 2010 (blue) and in the winter of 2010 (red).

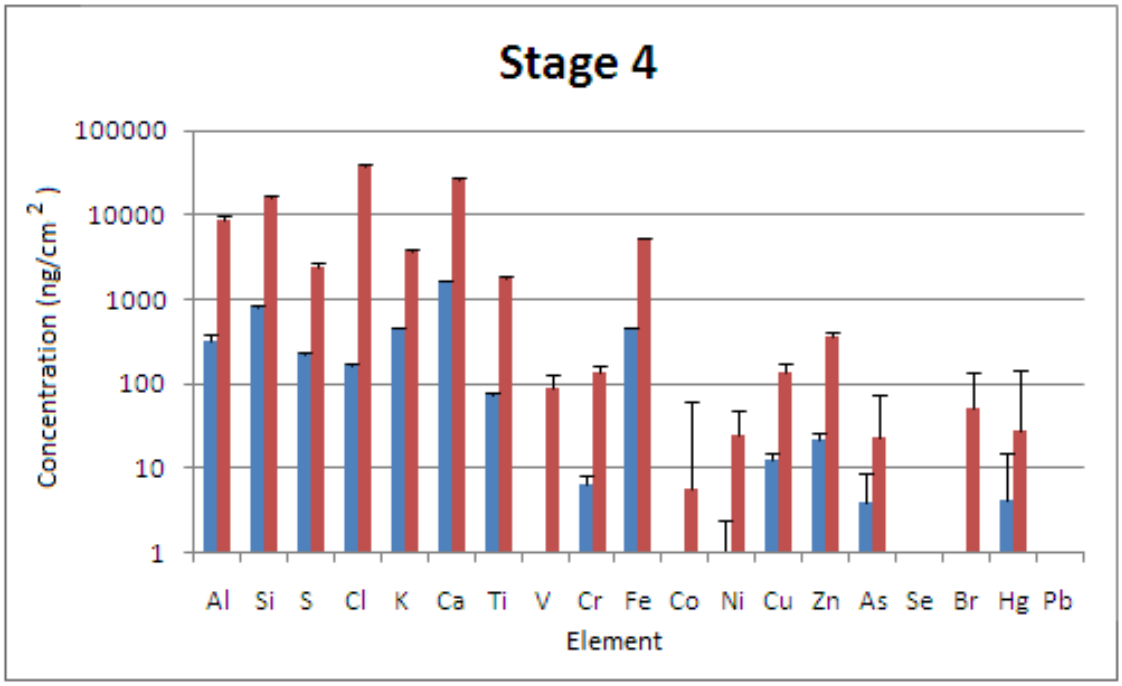

Figure 27: Bar graph comparing the elemental concentrations in ng/cm^{2}of aerosols with a diameter between 4-2 μm collected at Vale Cemetery in the summer of 2010 (blue) and in the winter of 2010 (red).

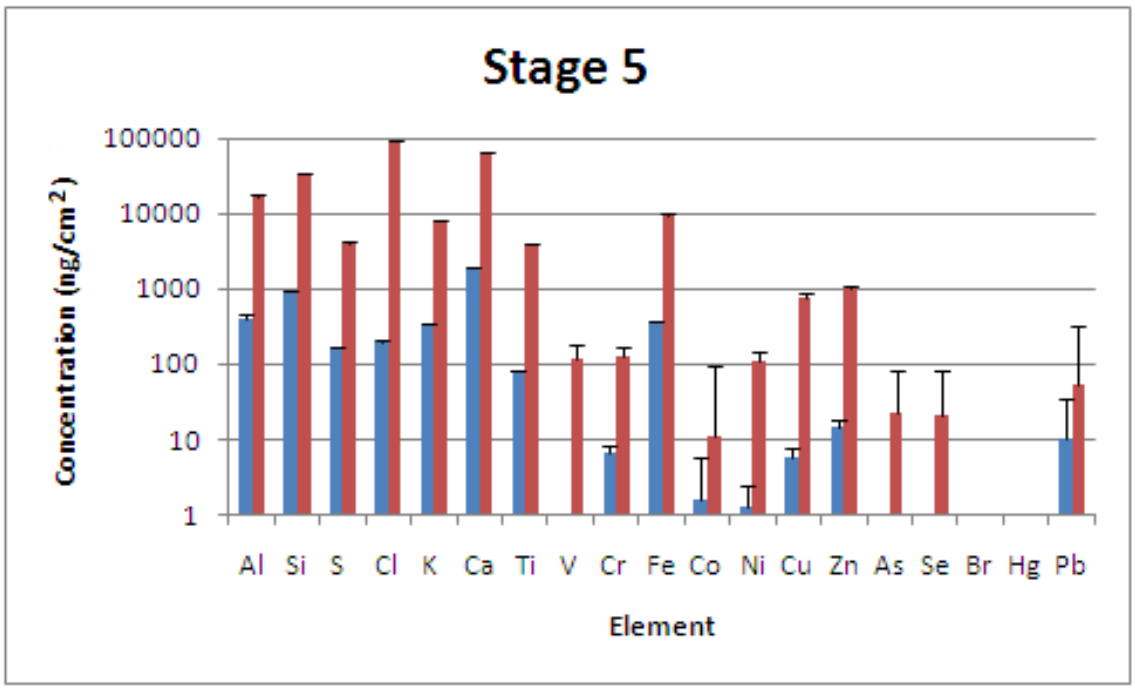

Figure 28: Bar graph comparing the elemental concentrations in ng/cm^{2}of aerosols with a diameter between 8-4 μm collected at Vale Cemetery in the summer of 2010 (blue) and in the winter of 2010 (red).

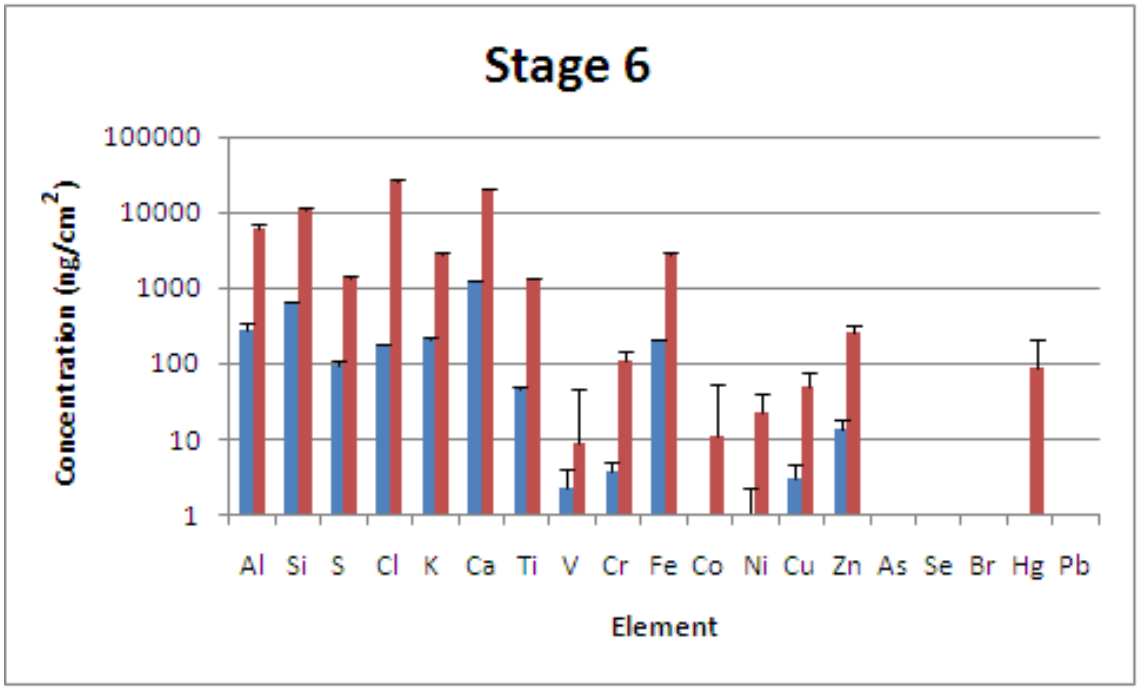

Figure 29: Bar graph comparing the elemental concentrations in ng/cm^{2}of aerosols with a diameter between 16-8 μm collected at Vale Cemetery in the summer of 2010 (blue) and in the winter of 2010 (red).

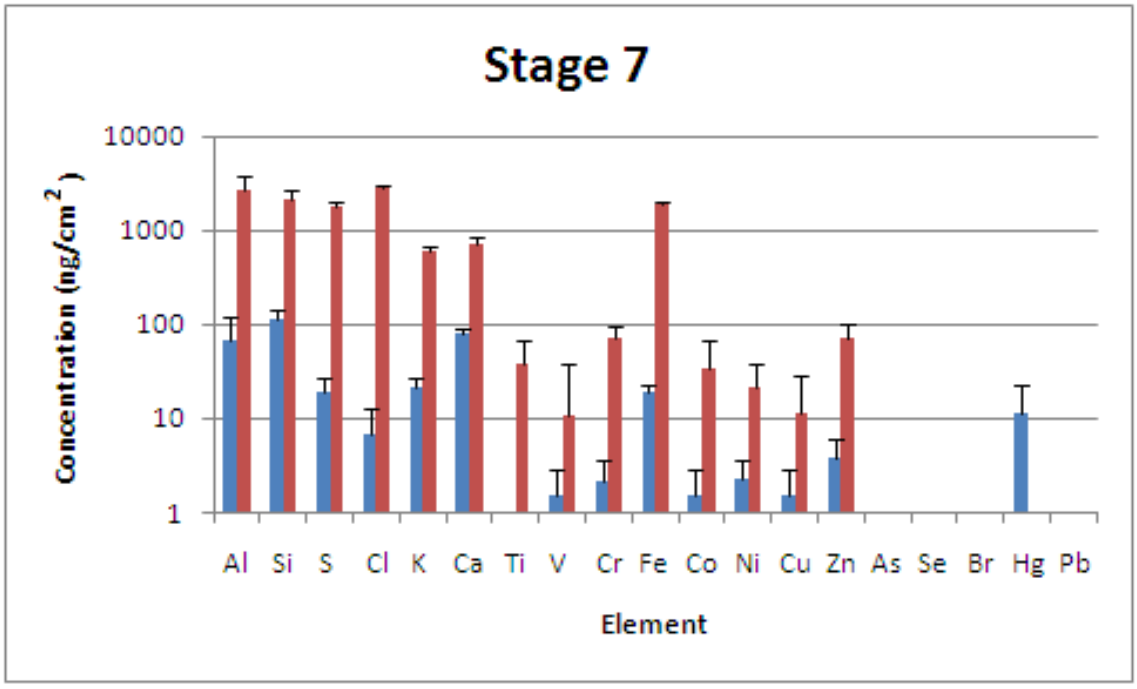

Figure 30: Bar graph comparing the elemental concentrations in ng/cm^{2}of aerosols with a diameter >16 μm collected at Vale Cemetery in the summer of 2010 (blue) and in the winter of 2010 (red).

Tables 5, 6, and 7 list the final elemental concentration determined for each element in ng/m^3. Shown in Figure 31 is a comparison of spectra taken on samples collected at Vale Cemetery in the summer of 2010 (blue) to the samples collected at Vale Cemetery in the winter of 2010 (red) for Stage 1 (particles range in diameter between 0.25-0.5 μm). Bar graphs comparing the elemental concentrations of samples collected at Vale Cemetery in the summer of 2010 (blue) to the winter of 2010 for all stages of the cascade impactor as a function of element are shown in Figures 32-40.

Table 5: Elemental concentrations for the samples collected at the Union College Boathouse.

Elemental Concentration (ng/m^3)						
Element	Stage 1 0.25-0.5μm	2 0.5-1	4 2-4	5 4-8	6 8-16	7 >16
Al	1.34 ±0.47	3.11 ±0.83	10.7 ±2.6	12.4 ±2.6	5.5 ±1.3	2.21 ±0.87
Si	1.98 ±0.44	6.5 ±1.2	34.7 ±7.9	44.3 ±8.4	19.6 ±3.8	5.7 ±1.1
S	31.6 ±6.3	15.2 ±2.6	8.4 ±1.9	7.44 ±1.42	1.97 ±0.39	0.5 ±0.1
Cl	0.24 ±0.07	0.55 ±0.12	3.17 ±0.72	2.81 ±0.54	0.72 ±0.16	0.19 ±0.09
K	0.95 ±0.19	1.19 ±0.21	18.0 ±4.1	18.14 ±3.43	4.91 ±0.94	1.55 ±0.30
Ca	0.72 ±0.15	2.27 ±0.39	31.2 ±7.0	46.4 ±8.8	22.6 ±4.3	7.4 ±1.4
Ti	0.03 ±0.01	0.18 ±0.04	1.38 ±0.31	1.61 ±0.31	0.59 ±0.12	0.11 ±0.03
Cr	0.02 ±0.01	0.06 ±0.02	0.12 ±0.04	0.16 ±0.04	0.07 ±0.03	0.02 ±0.02
Fe	0.63 ±0.13	3.44 ±0.60	25.5 ±5.8	25.4 ±4.8	7.7 ±1.5	1.17 ±0.23
Ni	0.02 ±0.01	0.01 ±0.01	0.12 ±0.04	0.03 ±0.02	0.02 ±0.02	0.02 ±0.02
Cu	0.07 ±0.02	0.12 ±0.03	0.58 ±0.14	0.32 ±0.08	0.06 ±0.03	0.01 ±0.02
Zn	0.27 ±0.06	0.08 ±0.03	0.94 ±0.22	0.70 .15	0.28 ±0.07	0.16 ±0.05
Se	0.06 ±0.04	0.07 ±0.05	0 -	0 -	0 -	0 -
Br	0.13 ±0.07	0.09 ±0.08	0.08 ±0.08	0 -	0 -	0 -
Pb	1.79 ±0.63	0.23 ±0.37	0.51 ±0.57	0 -	0 -	0 -

Table 6: Elemental concentrations for samples collected at Vale Cemetery during the summer of 2010.

Elemental Concentration (ng/m^3)									
Element	Stage L1	L2	1	2	3	4	5	6	7
Al	0.5 ±1.0	0.58 ±0.58	2.6 ±1.5	2.7 ±2.2	2.3 ±2.6	4.9 ±3.2	7.7 ±4.3	5.7 ±2.4	1.4 ±1.2
Si	0.40 ±0.79	0.43 ±0.42	4.6 ±1.8	3.1 ±2.6	4.4 ±4.8	12.4 ±7.7	18.4 ±9.8	12.7 ±4.9	2.3 ±1.0
S	0.49 ±0.96	0.58 ±0.56	50 ±20	7.1 ±5.9	2.5 ±2.8	3.5 ±2.2	3.3 ±1.7	1.94 ±0.75	0.37 ±0.21
Cl	0.25 ±0.49	0.34 ±0.33	7.3 ±2.8	0.22 ±0.18	0.76 ±0.84	2.5 ±1.6	3.9 ±2.1	3.5 ±1.3	0.14 ±0.12
K	0.6 ±1.1	0.68 ±0.66	25.5 ±10.0	0.76 ±0.62	1.8 ±2.0	7.0 ±4.3	6.7 ±3.6	4.1 ±1.6	0.43 ±0.19
Ca	0.34 ±0.67	0.47 ±0.46	3.4 ±1.3	2.0 ±1.7	6.2 ±6.9	26 ±16	37.2 ±19.8	24.8 ±9.4	1.56 ±0.64
Ti	0.02 ±0.03	0.01 ±0.01	0.20 ±0.08	0.20 ±0.16	0.35 ±0.39	1.15 ±0.72	1.57 ±0.84	0.94 ±0.36	0 -
V	0 -	0 -	0.04 ±0.03	0 -	0 -	0 -	0 -	0.04 ±0.04	0.03 ±0.03
Cr	0 -	0.01 ±0.01	0.05 ±0.03	0.03 ±0.03	0.05 ±0.05	0.10 ±0.07	0.14 ±0.08	0.07 ±0.04	0.04 ±0.03
Fe	0.07 ±0.14	0.1 ±0.09	1.41 ±0.55	1.2 ±1.0	2.8 ±3.1	6.9 ±4.3	7.3 ±3.9	4.0 ±1.5	0.37 ±0.16
Co	0 -	0 -	0.03 ±0.04	0 -	0 -	0 -	0.03 ±0.08	0 -	0.03 ±0.03
Ni	0 -	0 -	0.04 ±0.03	0.02 ±0.02	0 -	0.02 ±0.02	0.03 ±0.03	0.02 ±0.03	0.05 ±0.03
Cu	0.02 ±0.04	0 -	0.18 ±0.08	0.03 ±0.03	0.08 ±0.10	0.19 ±0.13	0.11 ±0.07	0.06 ±0.04	0.03 ±0.03
Zn	0.02 ±0.05	0.04 ±0.04	2.7 ±1.1	0.07 ±0.06	0.12 ±0.14	0.33 ±0.22	0.3 ±0.17	0.28 ±0.13	0.08 ±0.05
As	0 -	0 -	0 -	0 -	0.03 ±0.05	0.06 ±0.08	0 -	0 -	0 -
Se	0 -	0 -	0.09 ±0.11	0 -	0 -	0 ±0.08	0 -	0 -	0 -
Br	0 -	0 -	0.38 ±0.23	0.05 ±0.08	0 -	0 -	0 -	0 -	0 -
Hg	0 -	0 -	0 -	0 -	0 -	0.07 ±0.16	0 -	0 -	0.22 ±0.24
Pb	0 -	0 -	0.73 ±0.54	0.12 ±0.24	0 -	0 -	0.21 ±0.47	0 -	0 -

Table 7: Elemental concentrations for samples collected at Vale Cemetery during the Winter of 2010.

Elemental Concentration (ng/m^3)									
Element	Stage L1	L2	1	2	3	4	5	6	7
Al	13.6 ±8.8	9.4 ±6.2	11.0 ±7.0	7.6 ±5.1	18.6 ±10.7	39.6 ±20.4	225 ±124	83 ±47	36.0 ±24.1
Si	8.0 ±4.7	8.6 ±4.9	12.2 ±6.9	4.8 ±2.9	27.0 ±13.7	71.5 ±35.7	461 ±250	143.6 ±78.2	29.4 ±17.0
S	5.0 ±2.7	5.9 ±3.3	30 ±16	7.4 ±4.0	12.2 ±6.1	11.1 ±5.6	55.5 ±30.3	17.71 ±9.85	24.6 ±13.6
Cl	16.4 ±8.8	21.2 ±11.6	153 ±85	7.5 ±4.1	32.8 ±16.4	171 ±85	1235 ±669	349 ±190	37.3 ±20.4
K	13.2 ±7.1	17.4 ±9.6	114 ±64	12.9 ±7.0	8.11 ±4.07	16.9 ±8.4	107 ±58	37.5 ±20.4	8.17 ±4.54
Ca	0.43 ±0.72	0.3 ±0.6	2.7 ±1.5	0.38 ±0.56	35.2 ±17.6	119.6 ±59.5	879 ±477	273 ±148	9.54 ±5.46
Ti	0.35 ±0.23	0.1 ±0.1	0.35 ±0.22	0.13 ±0.11	3.04 ±1.53	8.11 ±4.04	53.1 ±28.8	17.99 ±9.78	0.53 ±0.50
V	0.11 ±0.13	0.03 ±0.09	0.01 ±0.09	0 -	0 -	0.39 ±0.26	1.6 ±1.2	0.12 ±0.48	0.15 ±0.37
Cr	0.27 ±0.18	0.19 ±0.13	0.34 ±0.21	0.17 ±0.12	0.29 ±0.18	0.60 ±0.33	1.7 ±1.1	1.52 ±0.91	0.95 ±0.60
Fe	0.63 ±0.39	0.23 ±0.18	1.70 ±0.96	0.28 ±0.19	7.3 ±3.6	23.7 ±11.8	131.3 ±71.2	38.5 ±20.9	25.1 ±13.7
Co	0.06 ±0.09	0.04 ±0.06	0 -	0 -	0 -	0.03 ±0.26	0.15 ±1.12	0.15 ±0.57	0.47 ±0.52
Ni	0.13 ±0.11	0.09 ±0.08	0.09 ±0.08	0 -	0.17 ±0.13	0.11 ±0.12	1.46 ±0.96	0.29 ±0.30	0.28 ±0.29
Cu	0.10 ±0.11	0.03 ±0.06	0.40 ±0.24	0 -	1.17 ±0.62	0.63 ±0.35	10.5 ±5.8	0.69 ±0.50	0.16 ±0.25
Zn	0.52 ±0.33	0.81 ±0.48	7.0 ±3.9	0.59 ±0.35	1.82 ±0.95	1.58 ±0.82	13.8 ±7.6	3.48 ±2.05	0.96 ±0.67
As	0 -	0 -	0 -	0 -	0 -	0.10 ±0.23	0.31 ±0.82	0 -	0 -
Se	0.2 ±0.3	0 -	0 -	0 -	0 -	0 -	0.29 ±0.81	0 -	0 -
Br	0 -	0 -	0.52 ±0.45	0.29 ±0.33	0 -	0.23 ±0.38	0 -	0 -	0 -
Hg	0 -	0 -	0 -	0 -	0.13 ±0.47	0.13 ±0.51	0 -	1.17 ±1.77	0 -
Pb	0 -	0 -	1.2 ±1.1	0 -	0.39 ±1.25	0 -	0.7 ±3.7	0 -	0 -

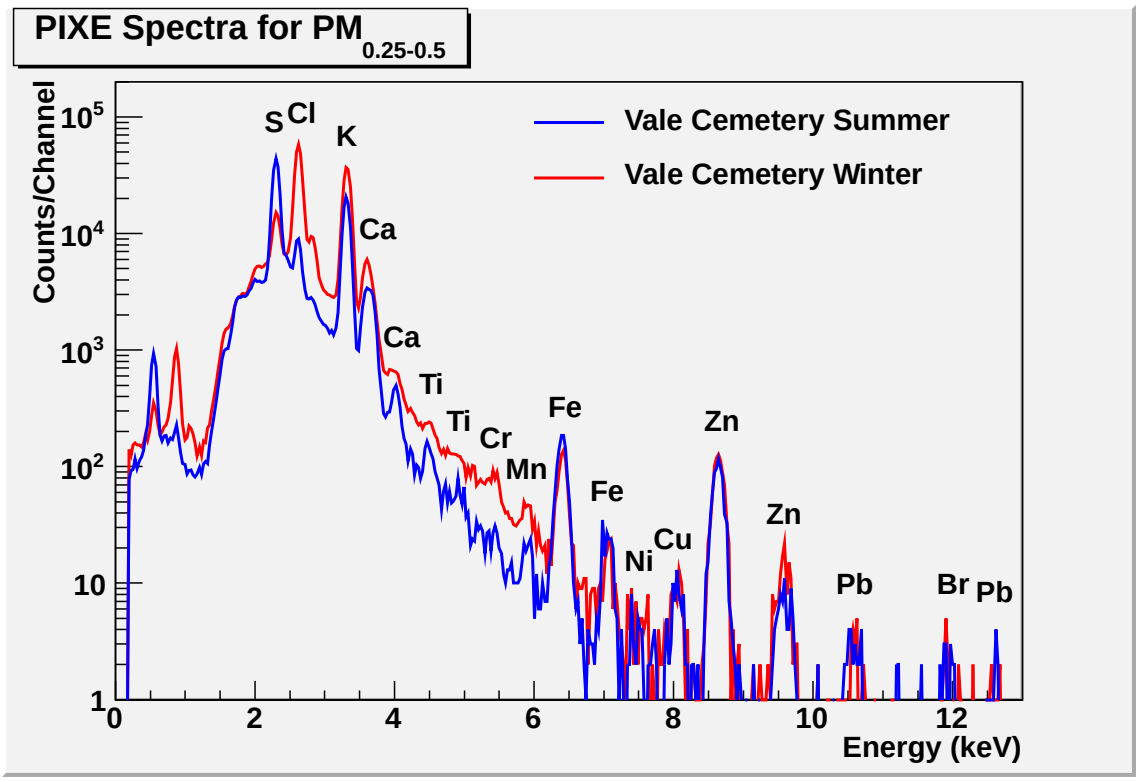

Figure 31: Comparison spectra between aerosols collected at Vale Cemetery in the summer of 2010 (blue) and the winter of 2010 (red).

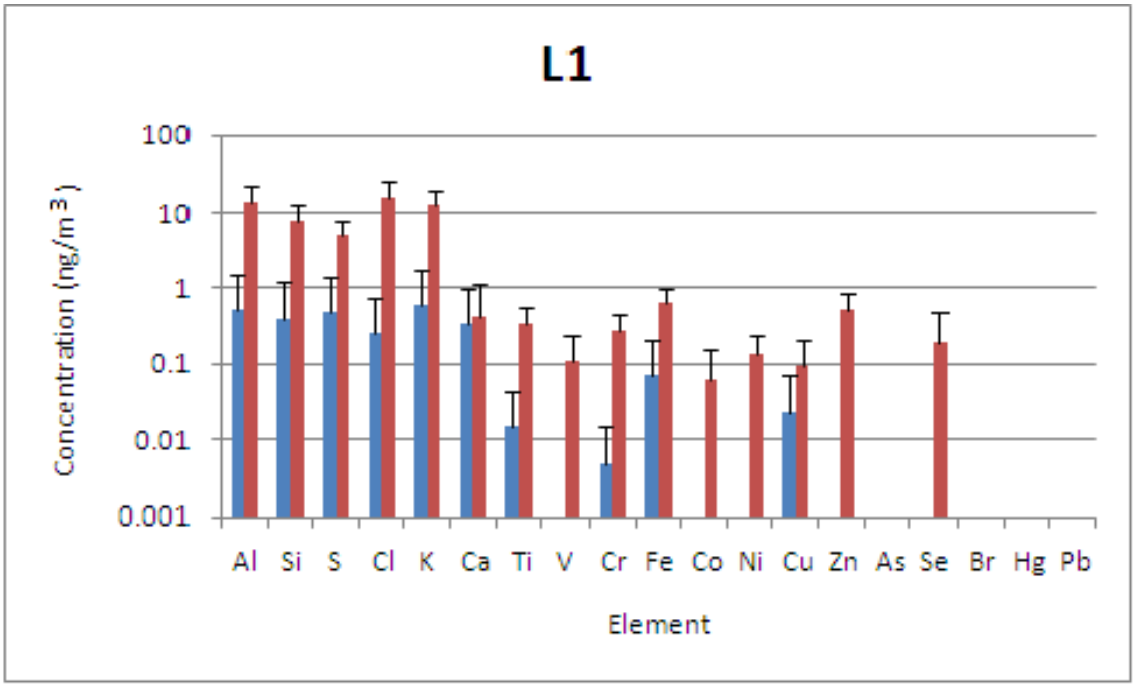

Figure 32: Bar graph comparing the elemental concentrations for aerosols in ng/m^3 with a diameter between 0.12-0.06 μm collected at Vale Cemetery in the summer of 2010 (blue) to the winter of 2010 (red).

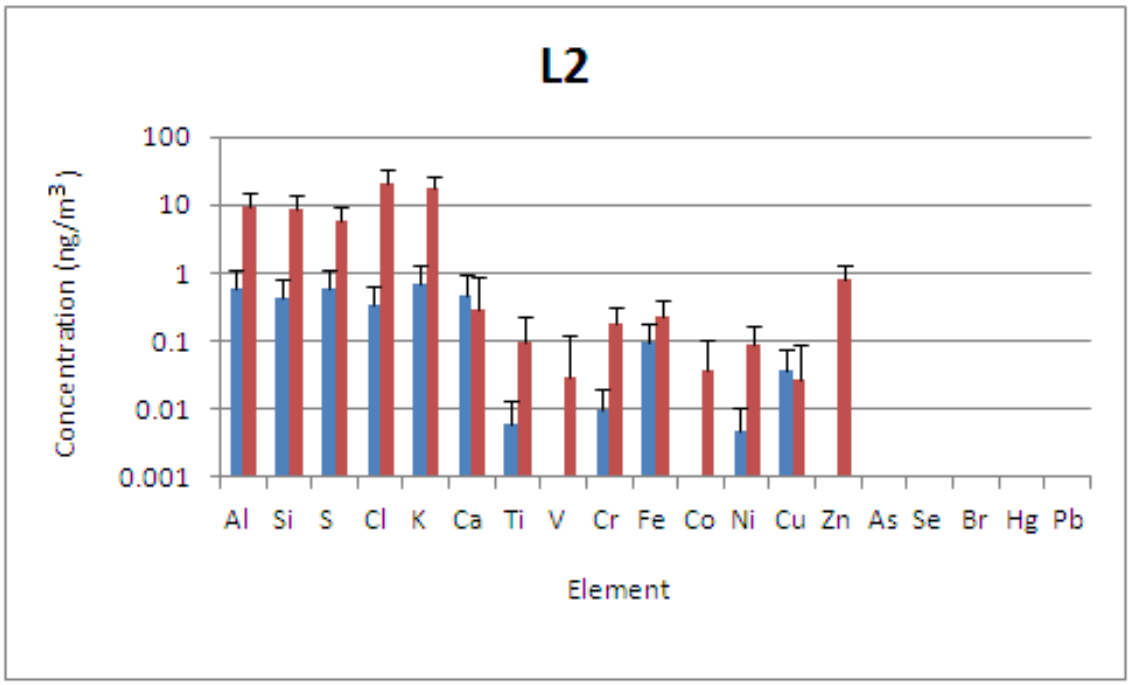

Figure 33: Bar graph comparing the elemental concentrations for aerosols in ng/m^3 with a diameter between 0.25-0.12 μm collected at Vale Cemetery in the summer of 2010 (blue) to the winter of 2010 (red).

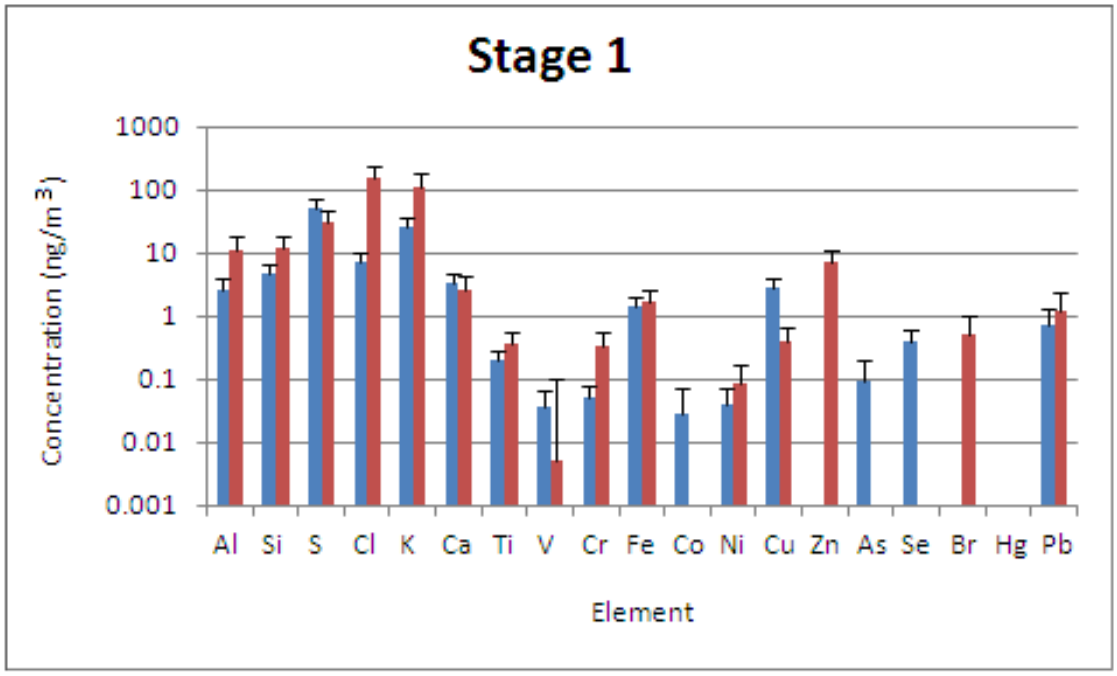

Figure 34: Bar graph comparing the elemental concentrations for aerosols in ng/m^3 with a diameter between 0.5-0.25 μm collected at Vale Cemetery in the summer of 2010 (blue) to the winter of 2010 (red).

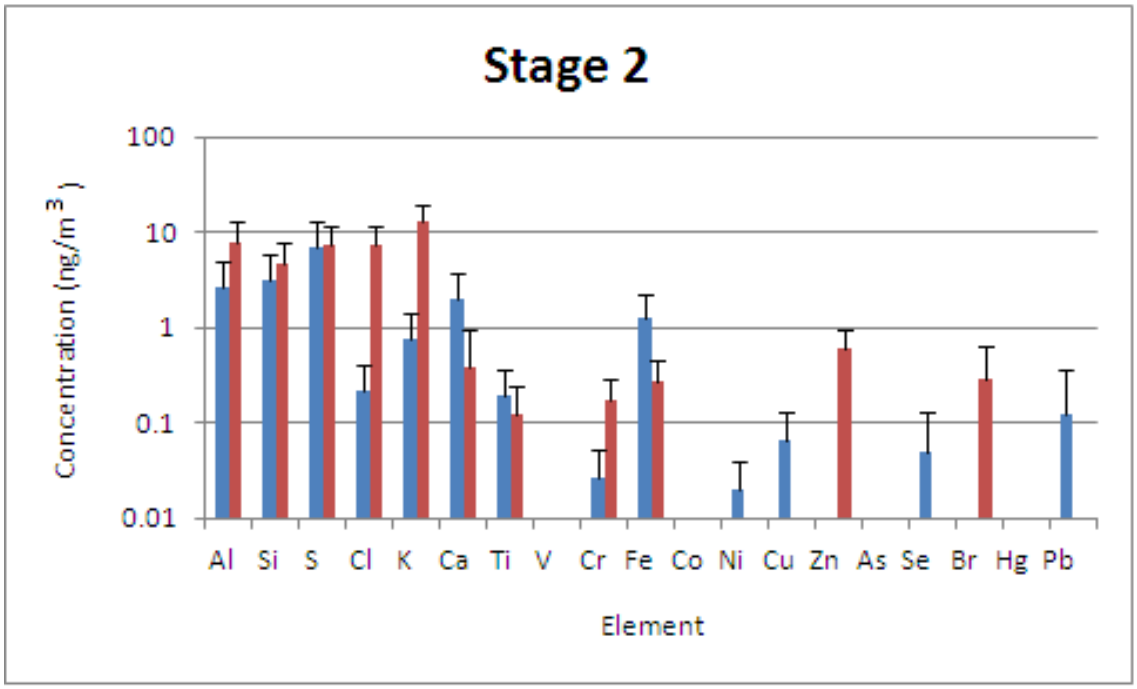

Figure 35: Bar graph comparing the elemental concentrations for aerosols in ng/m^3 with a diameter between 1-0.5 μm collected at Vale Cemetery in the summer of 2010 (blue) to the winter of 2010 (red).

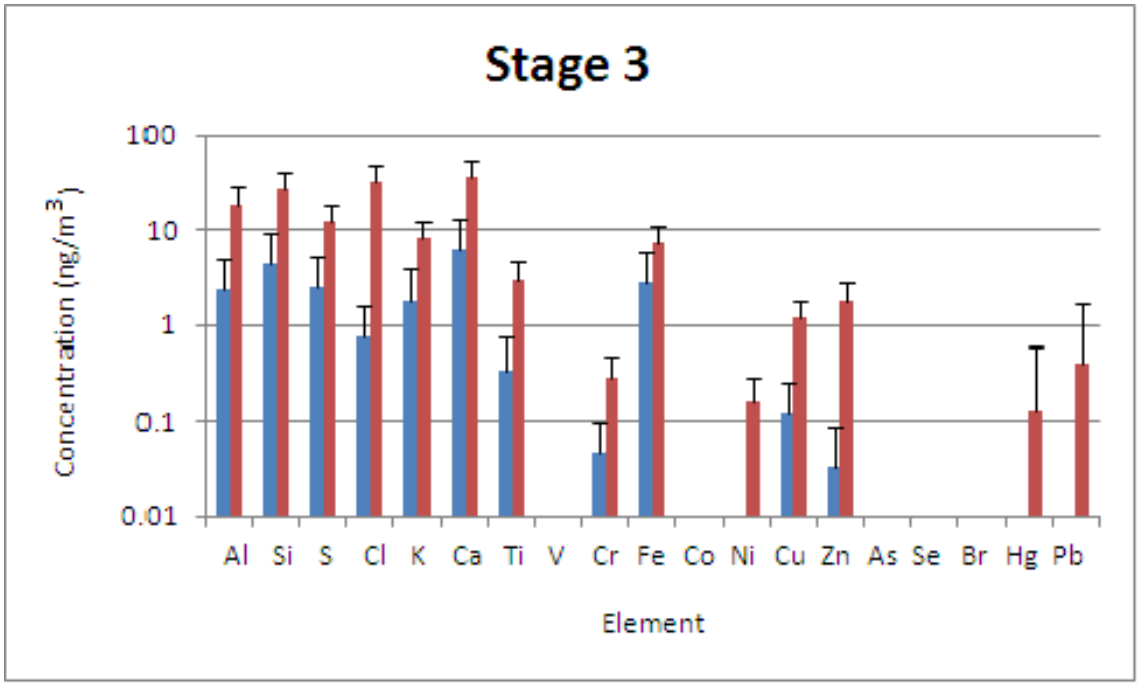

Figure 36: Bar graph comparing the elemental concentrations for aerosols in ng/m^3 with a diameter between 2-1 μm collected at Vale Cemetery in the summer of 2010 (blue) to the winter of 2010 (red).

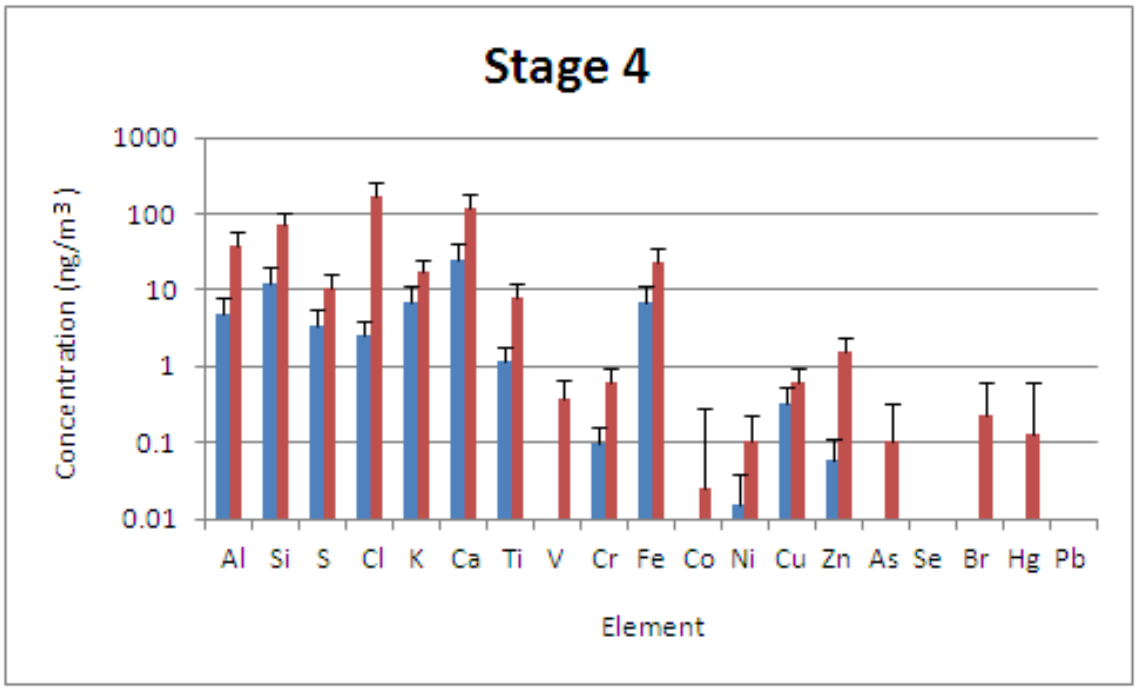

Figure 37: Bar graph comparing the elemental concentrations for aerosols in ng/m^3 with a diameter between 4-2 μm collected at Vale Cemetery in the summer of 2010 (blue) to the winter of 2010 (red).

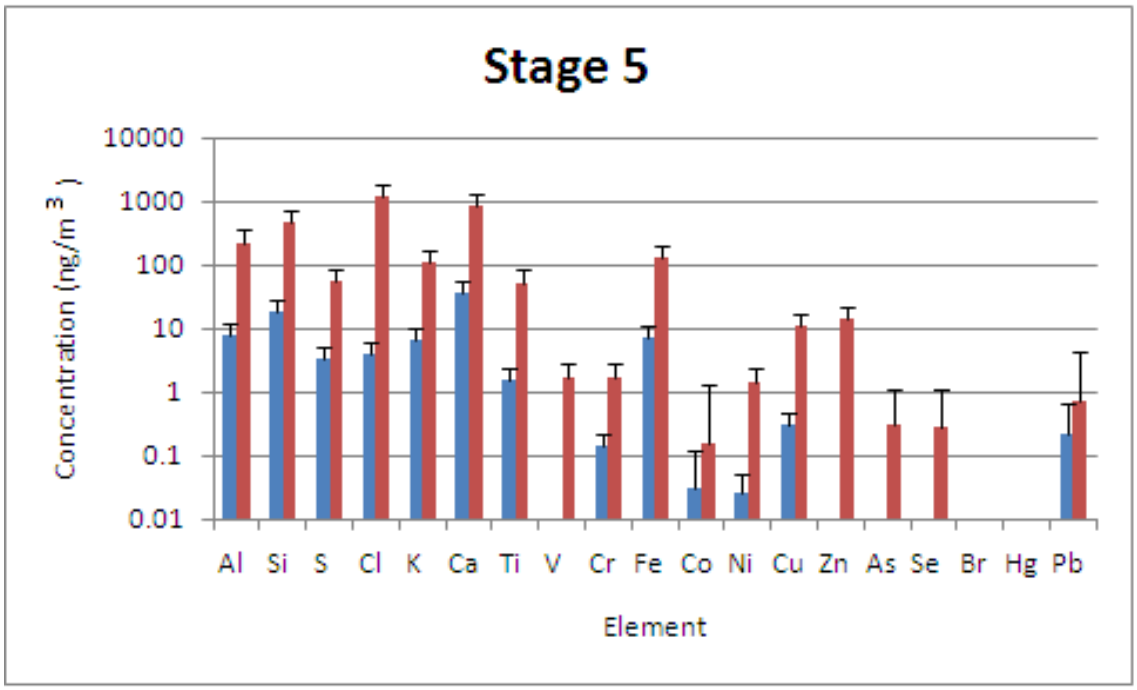

Figure 38: Bar graph comparing the elemental concentrations for aerosols in ng/m^3 with a diameter between 8-4 μm collected at Vale Cemetery in the summer of 2010 (blue) to the winter of 2010 (red).

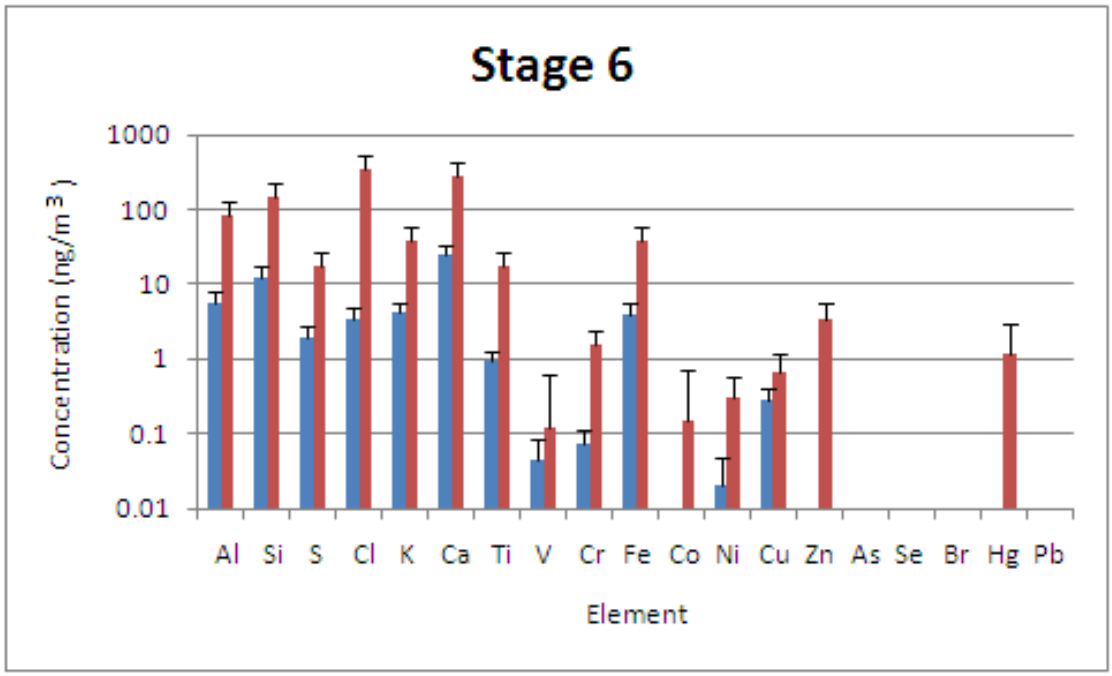

Figure 39: Bar graph comparing the elemental concentrations for aerosols in ng/m^3 with a diameter between 16-8 μm collected at Vale Cemetery in the summer of 2010 (blue) to the winter of 2010 (red).

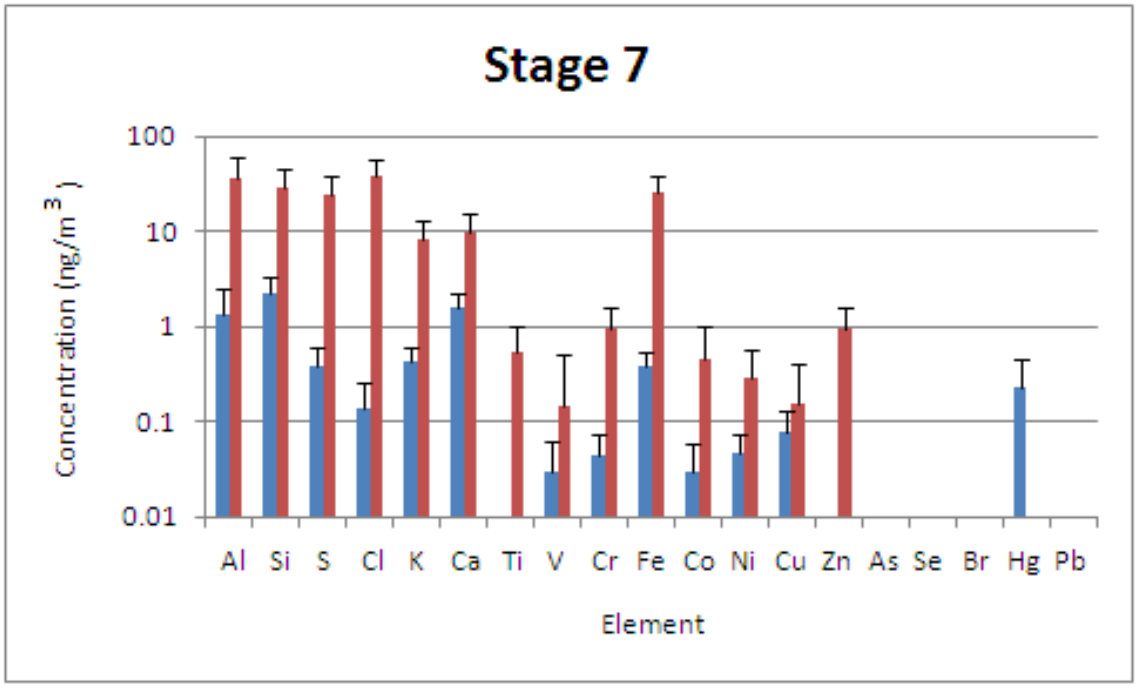

Figure 40: Bar graph comparing the elemental concentrations for aerosols in ng/m^3 with a diameter >16 μm collected at Vale Cemetery in the summer of 2010 (blue) to the winter of 2010 (red).

These graphs highlight seasonal differences for aerosols collected at the same location. The samples collected in the winter of 2010 generally have higher elemental concentrations than those collected in the summer with a few exceptions. The exact reason why there is a higher concentration is not completely understood. It could be as simple as seasonal changes mean higher concentrations, but there could be other factors. During sample collection in the summer, there were problems with keeping the flow rate to consistently remain at 1 L/min. I attempted to account for this, but since the flow rate could not continuously be monitored, it is hard to determine by how much the flow rate changed. The comparison graph of Stage 2 makes interpreting these results more difficult because there are summer concentrations equal and even surpassing those of the winter samples. Another reason why higher elemental concentrations occurred in the winter samples could be due to the fact that the proton beam was not completely centered on the deposit of the summer samples.

Figures 41 shows a comparison of spectra taken on aerosols collected at Vale Cemetery during the summer of 2010 to samples collected at the Union College Boathouse during the summer of 2009. Shown in Figures 42-47 are bar graphs comparing the elemental concentrations in ng/m^3 of samples collected at Vale Cemetery in the summer of 2010 to samples collected at the Union College Boathouse in the Summer of 2009.

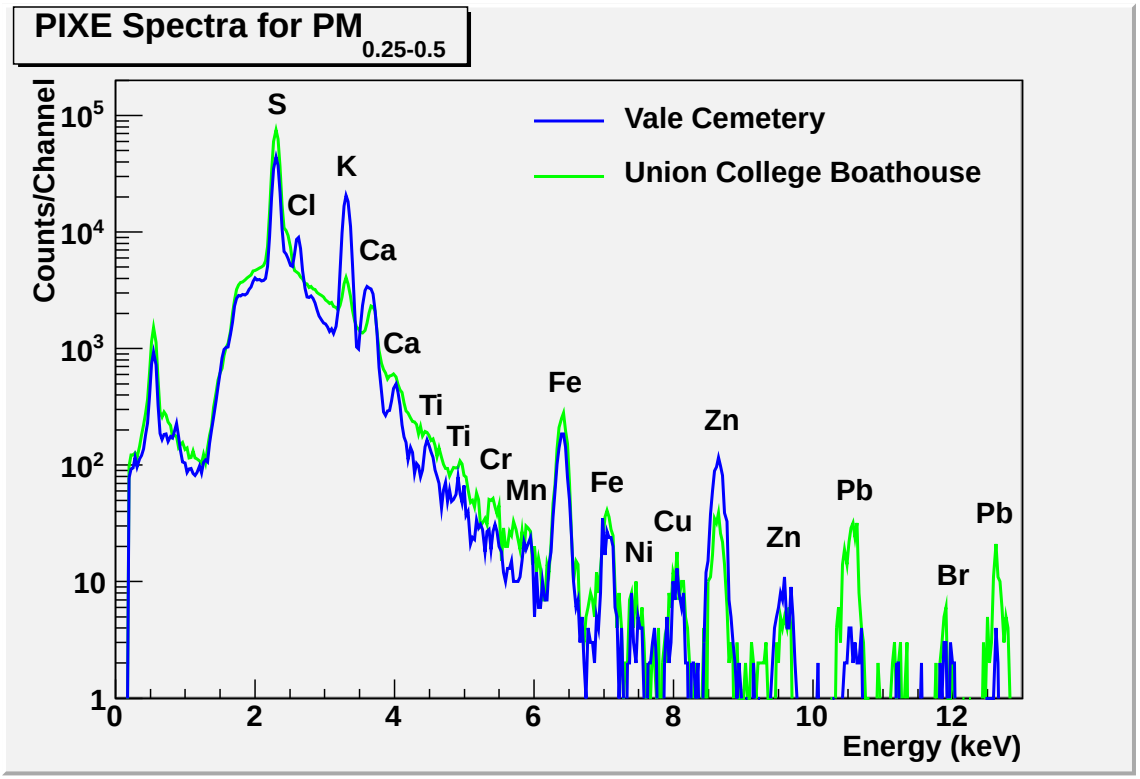

Figure 41: Comparison spectra for aerosols collected at Vale Cemetery during the summer of 2010 (blue) to aerosols collected at the Union College Boathouse during the summer of 2009 (green).

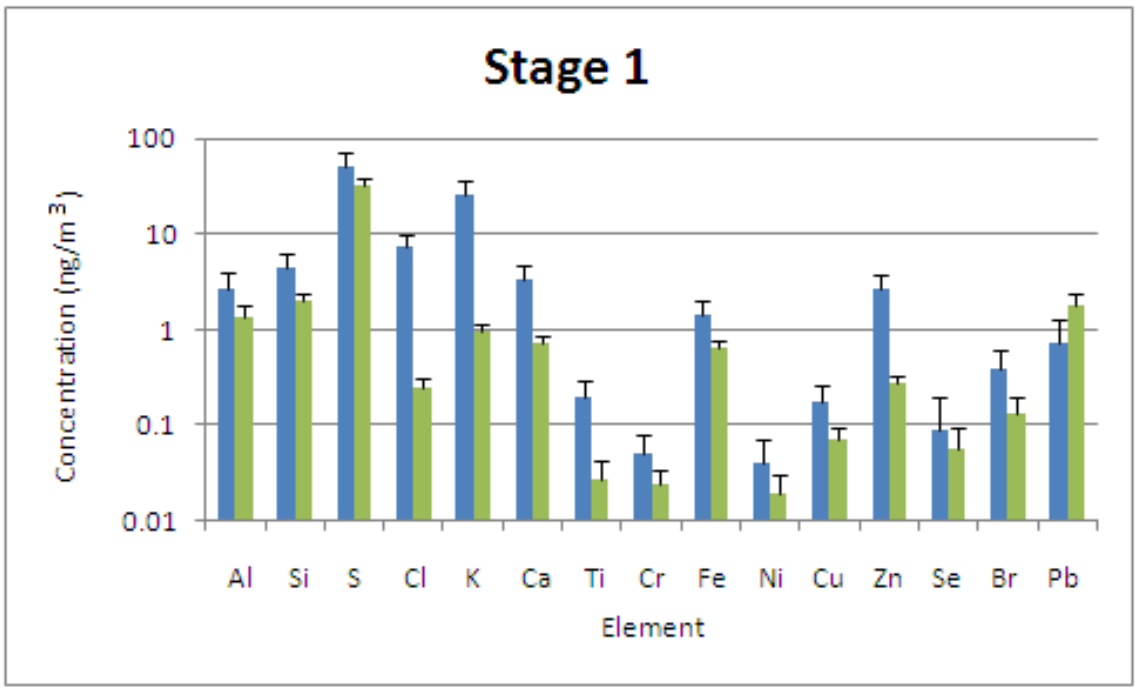

Figure 42: Bar graph comparing the elemental concentrations in ng/cm^{3}of aerosols with a diameter between 0.5-0.25 μm collected at Vale Cemetery in the summer of 2010 (blue) to the Union College Boathouse (green).

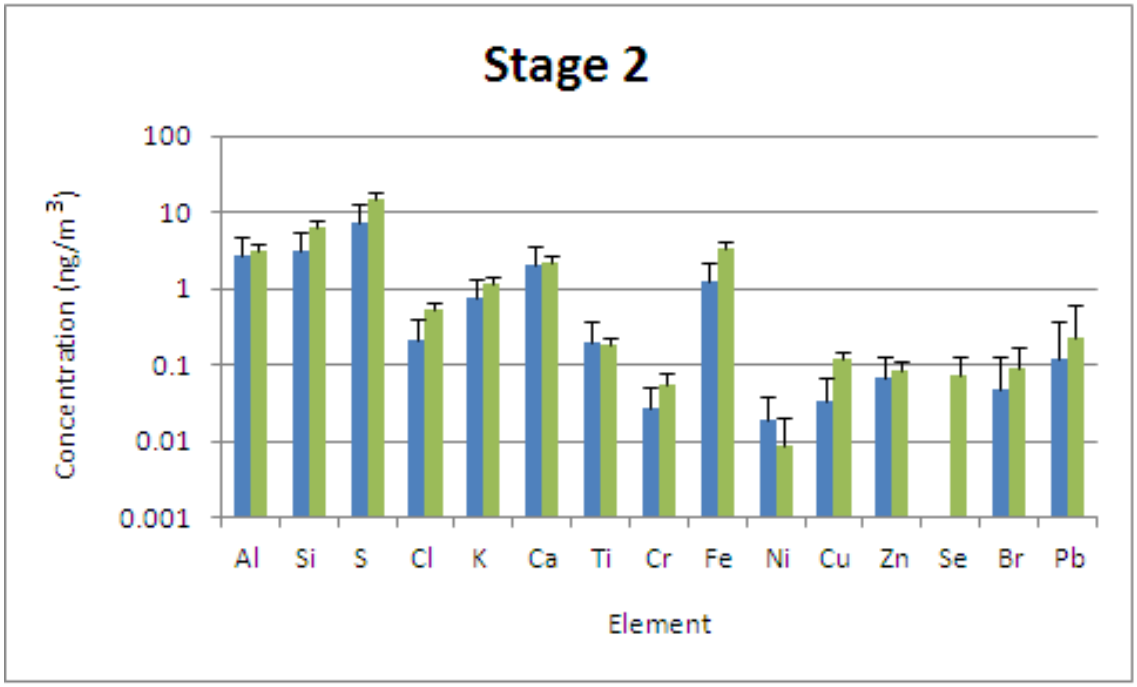

Figure 43: Bar graph comparing the elemental concentrations in ng/cm^{3}of aerosols with a diameter between 1-0.5 μm collected at Vale Cemetery in the summer of 2010 (blue) to the Union College Boathouse (green).

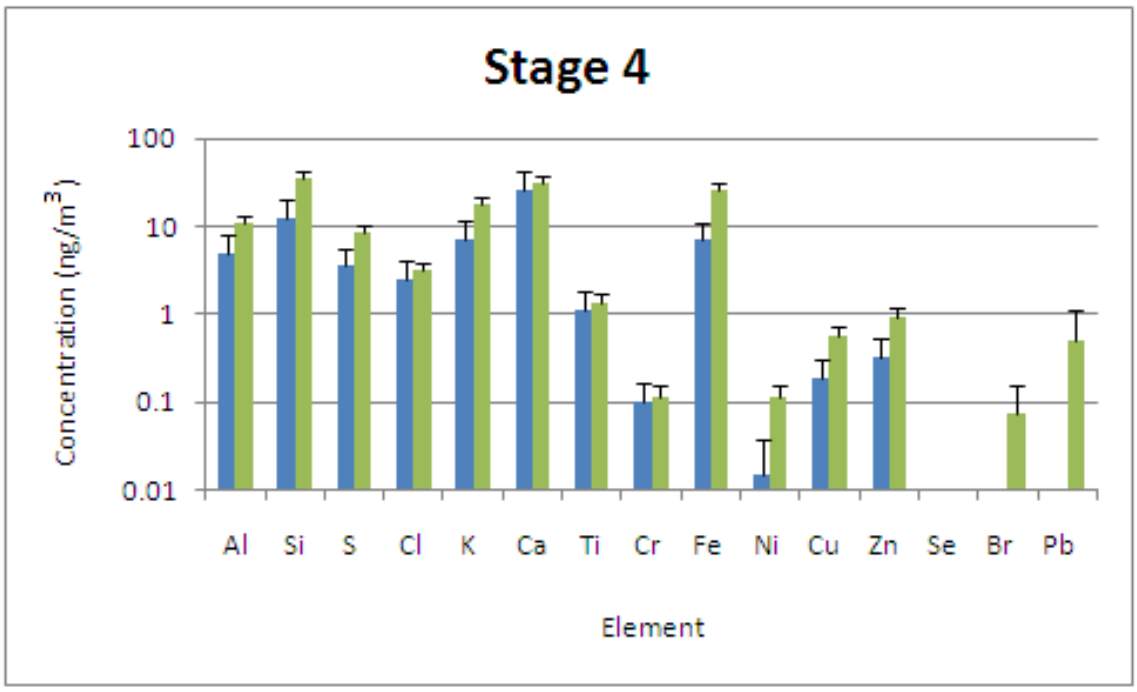

Figure 44: Bar graph comparing the elemental concentrations in ng/cm^{3}of aerosols with a diameter between 4-2 μm collected at Vale Cemetery in the summer of 2010 (blue) to the Union College Boathouse (green).

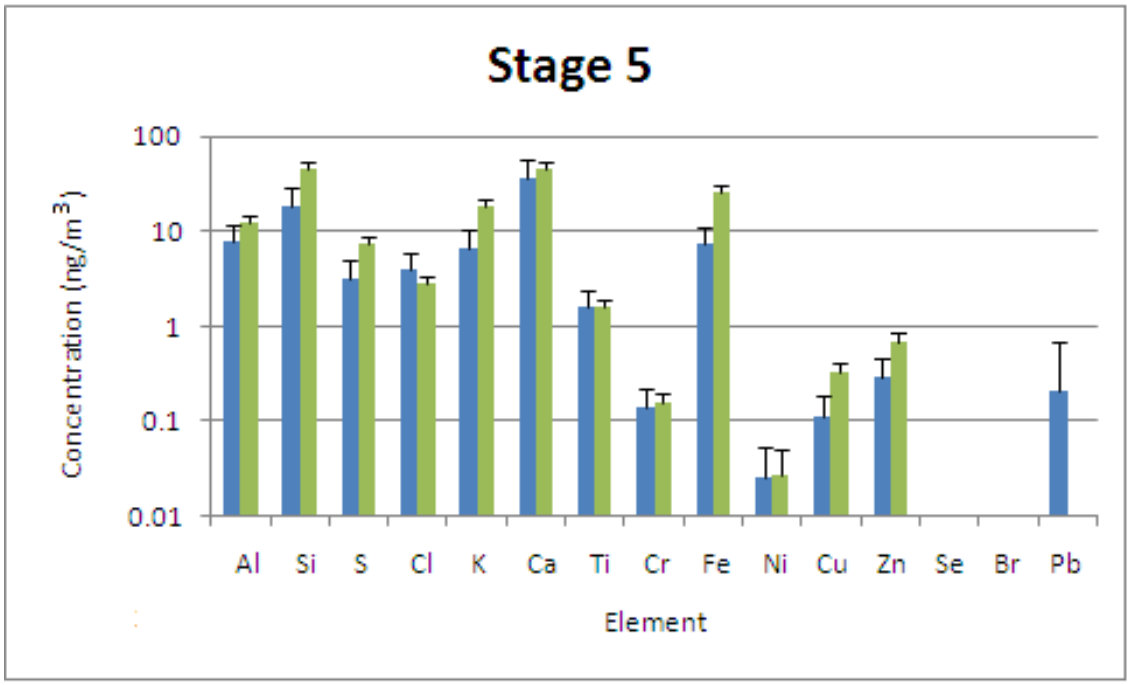

Figure 45: Bar graph comparing the elemental concentrations in ng/cm^{3}of aerosols with a diameter between 8-4 μm collected at Vale Cemetery in the summer of 2010 (blue) to the Union College Boathouse (green).

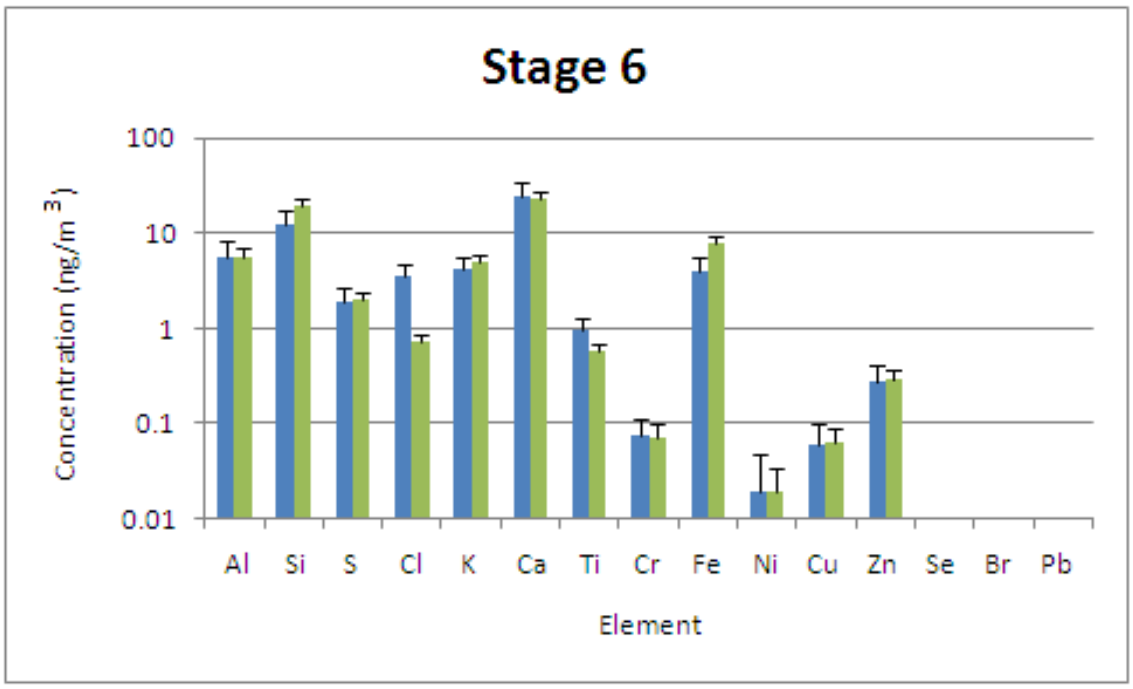

Figure 46: Bar graph comparing the elemental concentrations in ng/cm^{3}of aerosols with a diameter between 16-8 μm collected at Vale Cemetery in the summer of 2010 (blue) to the Union College Boathouse (green).

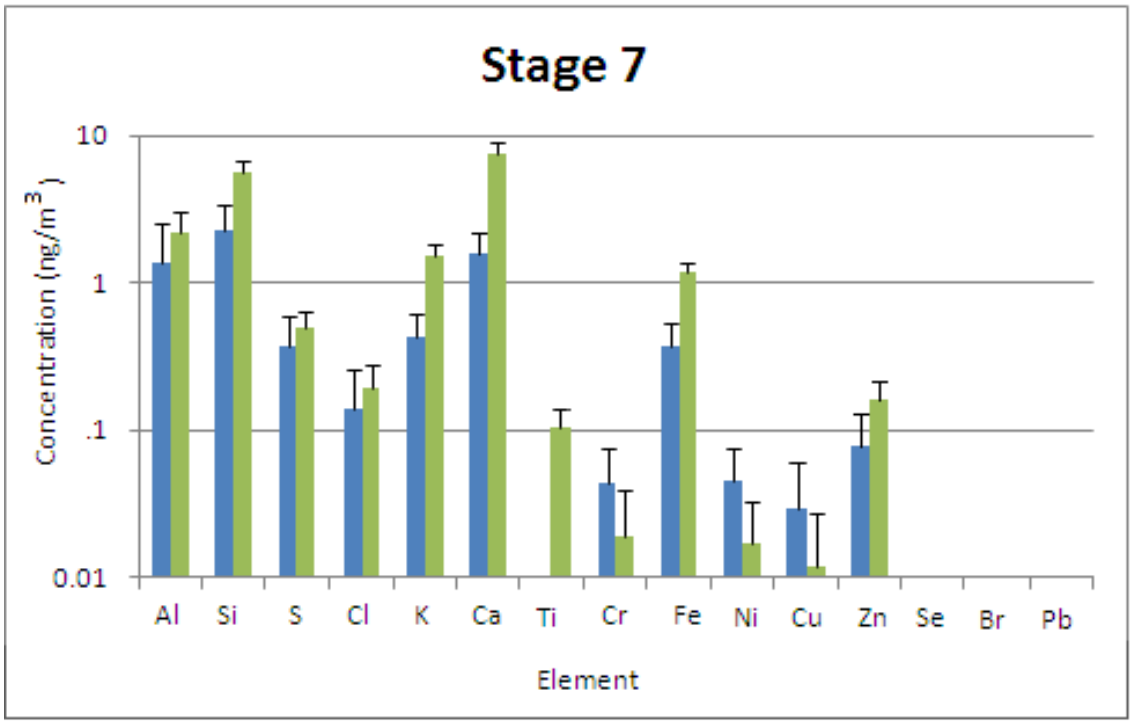

Figure 47: Bar graph comparing the elemental concentrations in ng/cm^{3}of aerosols with a diameter >16 μm collected at Vale Cemetery in the summer of 2010 (blue) to the Union College Boathouse (green).

These graphs highlight seasonal differences for aerosols as well as differences in location. The Union College Boathouse is located in a more industrial area, along a river, and near railroad tracks. The impactor was also located close to the ground next to the Boathouse. The samples from Vale Cemetery were collected on the roof of the crematorium and further away from industrial processes than the Union College Boathouse samples. Some of the major differences between the samples are generally more iron, sulfur, and potassium in the Boathouse aerosols and more chlorine in the Vale Cemetery samples.

The error bars shown in Figures 32-47 were determined by adding the various uncertainties of quantities in Equations (1) and (2) together in quadrature. Each constant in Eq. (1) such as the H-value, the detector efficiency, and charge integrator all have small uncertainties all need to be taken into account. Quantities in

Eq. (2) such as the flow rate, temperature, and pressure vary throughout the total sampling time and those fluctuations need to be taken into account. Some examples of uncertainties used were around 5% for the H-value and 0.1 L/min for the flow rate. Furthermore, the area of the deposit, the concentration in ng/cm^2, and total sampling time all have their own uncertainties.

One goal is to be able to identify possible sources of pollution seen in our aerosol samples. For example, sulfur is one of the main byproducts of industrial processes and coal combustion [9]. This could possibly be a reason why there is more sulfur seen at the Boathouse, with the exception of Stage 1, than at Vale Cemetery as the Union College Boathouse is in a more industrial area and near railroad tracks. Other elements that are seen more consistently at the Union College Boathouse are silicon and iron, which make up a large proportion of soil [9]. Since the impactor was closer to the ground at the Union College Boathouse, it could have collected more wind blown soil than the impactor on the roof of Vale Cemetery. These source identification profiles developed by Cohen allow for a better understanding of why certain aerosols are present in different spectra [9].

An element that consistently appears in large quantities in both Vale Cemetery samples is chlorine, which peaks at (1235 ± 669) ng/m^{3}on Stage 5 of the Union College Boathouse samples. Cohen et. all list Cl as one of the main elements in sea spray [9]. This makes sense because sea spray would mainly consist of salt water, where chlorine is a main component. They also list Cl as being a part of smoke but at very small percentages (~1-5%); yet for Stage 5 Cl makes up ~39% of the total concentration. The rest of the source could come from salt water in the human body that was cremated, but that probably would not make up the rest of the difference. One thing I had speculated was that Cl is used in the embalming process to help sanitize the body. However, a quick search revealed that Cl is not used in the sanitizing process but rather a mixture of formaldehyde, glutaraldehyde, or phenol is used and those

chemicals do not contain any Cl [10]. Another observation is that Cl consistently appears in larger concentrations in the winter samples when compared to the summer samples. One explanation for this could be the Cl from road salt that dissolved and evaporated, thus becoming airborne.

As mentioned in the Introduction, two specific elements of interest in this thesis were mercury and lead. For lead, the goal was to determine if lead was actually present in the samples and, if so, to be able to determine if it fell below the new standards set by the EPA. While we did see lead in some of the samples, it was in very low amounts, peaking at (1.79 $\pm$ 0.63) ng/m^{3}for Stage 1 of the Union College Boathouse samples, well below the new EPA limits. According to the study led by Cohen, lead can be found in emissions from motor vehicles (~10%) and from industrial processes (~1%) [9]. Since the impactor was at a more industrial area and closer to traffic than at Vale Cemetery, it would make sense that the highest concentration of lead was seen at the Union College Boathouse.

Mercury was specifically studied in the crematorium emissions, as studies have shown that mercury amalgam fillings release mercury during the cremation process. Mercury, like lead, was also seen sparingly, with a maximum seen at (1.17 $\pm$ 1.77) ng/m^3 for Stage 6 of the winter 2010 samples taken at Vale cemetery. The large uncertainty begs the question of whether or not any mercury was actually seen at all in the sample. This large uncertainty makes it safe to say that there was essentially no mercury preset in the samples.

6 Summary

A comparative study of atmospheric aerosols was performed using PIXE in the Union College Ion-Beam Analysis Laboratory. Comparisons were made of samples collected at the Vale Cemetery crematorium in the summer of 2010 to samples collected at

the crematorium in the winter of 2010 and to samples collected at the Union College Boathouse during the summer of 2009. The purpose of this work was to identify any seasonal and locational similarities and differences between the samples, identify possible sources of pollution, and search for any heavy metals that may be toxic. The aerosols were collected using a nine stage cascade impactor and analyzed using the Union College Pelletron Accelerator.

One of the main byproducts of industrial processes is sulfur from coal combustion. The Union College Boathouse, where sulfur was consistently seen in greater quantities, is located in a more industrial area than the Vale Cemetery crematorium. This and the fact that the Boathouse is located near railroad tracks could be a possible explanation for why higher quantities of sulfur were seen there. Iron and silicon, elements that make up large proportions of soil, were also seen in larger quantities at the Union College Boathouse. One possible explanation for this is that the impactor was closer to the ground than at the crematorium, where it was on the roof. Toxic metals such as mercury and lead were seen in very low quantities and with large uncertainties, which makes it hard to determine if they were actually present in the sample.

The UCIBAL is developing a comprehensive ion-beam analysis research program for atmospheric aerosols. PIXE, with its wide range of elemental detection combined with high sensitivities and low detection limits, is the work horse IBA technique, but complementary IBA techniques such as PIGE, PESA, and RBS are being developed. Each of these research programs are still in there development phase, with many improvements soon to be added. The main improvement is the addition of a new scattering chamber, which will allow for simultaneous analysis of PIXE, PIGE, PESA, and RBS on the same sample at the same time. This latest apparatus will allow the UCIBAL to continue to produce exciting results and provide a great opportunity for future student researchers to participate in inspiring research.

References

[1] "NASA - Aerosols May Drive a Significant Portion of Arctic Warming." NASA - Home. Web. 28 Feb. 2011. <http://www.nasa.gov/topics/earth/features/warming_aerosols_prt.htm>.

[2] "EPA Tightens Limit on Airborne Lead - USATODAY.com." News, Travel, Weather, Entertainment, Sports, Technology, U.S. & World - USATODAY.com. Web. 28 Feb. 2011. <http://www.usatoday.com/news/health/2008-10-16-epa-lead_N.htm>.

[3] Reindl, John. "Summary of References on Mercury Emissions from Crematoria." 3 Nov. 2008. Web. <http://www.ejnet.org/crematoria/reindl.pdf>

[4] Johansson, Sven, John Campbell, and Klas Malmqvist. Particle Induced X-Ray Emission Spectrometry (PIXE). New York, NY: John Wiley & Sons, 1995.

[5] PIXE International Corporation, P.O. Box 2744, Tallahassee, FL 32316 U.S.A.

[6] Amptek Inc., 14 DeAngelo Drivem Bedford, MA, 01730, USA. <http://www.amptek.com/drift.html>

[7] MicroMatter Co., 18218 18th Ave. NW, Arlington, WA 98223, U.S.A.

[8] GUPIX, the versatile PIXE spectrum fitting software, University of Guelph.

[9] Cohen, David, Grahame Bailey, and Ramesh Kondepudi. "Elemental analysis by PIXE and other IBA techniques and their application to source fingerprinting of atmospheric fine particle pollution." Nuclear Instruments and Methods in Physics Research B. 109/110. (1996): 218-226. Print.

[10] http://en.wikipedia.org/wiki/Embalming_chemicals